

1 **Authors' responses to comments of reviewer # 2**

2 Referee's comment:

3 General Comments

4 I would like to acknowledge the work that the authors put into this updated manuscript version.
5 The addition of the new figure one combined with the edits made to the text creates a manuscript
6 that is an improved read throughout and the work put into the this updated version address the
7 majority of my issues from the first version. My main issue of how dense the text of the first
8 manuscript version I feel is resolved.

9 The second main issue I had with lack of data is nearly resolved and I greatly appreciate the
10 additional information in Table Two. This is a very critical bit of information in evaluating the
11 results presented in this paper. While I'm happy to see this information, I do think there needs to
12 be some explaining in the methods section as to where the data came from, particularly the data
13 collected at the field site. For the data from other field sites, a simple justification of similarity I
14 think is called for.

15 Authors' response:

16 *A brief discussion on site measurements for foliar nutrient contents and on other data measured*
17 *at similar sites which were used for corroborating modelled results in Table 2 are now included*
18 *(lines 353-363 in the revised manuscript).*

19 Referee's comment:

20 A comparison of the site's climate data would be great. Right now, the information in Table Two
21 just comes up.

22 Authors' response:

23 *Since Table 2 shows the effects of WTD drawdown on carbon and nutrient cycling, we have now*
24 *included a comparison of both modelled and measured growing season WTD between 2004 and*
25 *2009 at the beginning. This gives the readers a clear picture of how gradually drier weather*
26 *from 2004 to 2009 caused a growing season water table drawdown at the very beginning of the*
27 *Table 2 and hence facilitates a smoother progression to what follows next. We, however, did not*
28 *include comparison of weather variables such as temperature, precipitation etc. in Table 2 since*
29 *those are already presented in Table 1 and in Figures 7d, and 7h.*

30 Referee's comment:

31 In both Tables One and Two, I would like to see confidence intervals (or similar) of the
32 regression statistics (Table One) and modeled/measured parameters (Table Two). Using
33 approximations or ~ signs is enough here.

34 Authors' response:

35 *Standard errors are now added to regression statistics in Table 1 and other parameters*
36 *(wherever applicable) in Table 2 instead of approximation signs (~).*

37 Referee's comment:

38 In the Author's Response you say "The internal peat biogeochemistry and peatland nutrient
39 cycling modelled in ecosys are tested against leaf nitrogen concentrations, N mineralization,
40 rooting depth, GPP, and Re measured/estimated at either our site or at sites that had similar peat
41 substrates, hydrology and/or plant functional types." I don't see evidence of statistics showing
42 they were tested, only compared.

43 Authors' response:

44 *The comparisons between the modelled and measured (either at the site or at similar sites)*
45 *parameters in Table 2 were basically one to one bases and hence no statistical test was*
46 *performed on any of those comparisons. These comparisons facilitated further corroboration of*
47 *the modelled eco-hydrology and biogeochemistry processes that were rigorously tested against*
48 *hourly fluxes in Table 1 and also compared against daily, seasonal and annual estimates of EC-*
49 *derived NEP, GPP and R_e in Figures 3 through 8. The confusion is now clarified in lines 353-*
50 *356 of the revised manuscript.*

51 **Coupled eco-hydrology and biogeochemistry algorithms enable simulation of water table**
52 **depth effects on boreal peatland net CO₂ exchange**

53

54 Mohammad Mezbahuddin*^{1,2}, Robert F. Grant², and Lawrence B. Flanagan³

55

56 ¹*Environmental Stewardship Branch, Alberta Agriculture and Forestry, Edmonton, AB, Canada*

57 ²*Department of Renewable Resources, University of Alberta, Edmonton, AB, Canada*

58 ³*Department of Biological Sciences, University of Lethbridge, AB, Canada*

59

60 *corresponding author. Email addresses: symon.mezbahuddin@gov.ab.ca,

61 mezbahud@ualberta.ca.

Abstract

Water table depth (WTD) effects on net ecosystem CO₂ exchange of boreal peatlands are largely mediated by hydrological effects on peat biogeochemistry, and eco-physiology of peatland vegetation. Lack of representation of these effects in carbon models currently limits our predictive capacity for changes in boreal peatland carbon deposits under potential future drier and warmer climates. We examined whether a process-level coupling of a prognostic WTD with 1) oxygen transport which controls energy yields from microbial and root oxidation-reduction reactions, and 2) vascular and non-vascular plant water relations could explain mechanisms that control variations in net CO₂ exchange of a boreal fen under contrasting WTD conditions i.e. shallow vs. deep WTD. ~~whether This coupling of eco-hydrology and biogeochemistry algorithms in a process-based ecosystem model *ecosys* could simulate~~ was tested against net ecosystem CO₂ exchange ~~measurements of in~~ a Western Canadian boreal fen peatland over a period of drier weather driven gradually deepening water table WTD drawdown due to drier weather from 2004 to 2009. ~~The goal was to test whether a process-level coupling of a prognostic WTD with 1) oxygen transport which controls energy yields from microbial and root oxidation-reduction reactions, and 2) vascular and non-vascular plant water relations could explain mechanisms that control variations in net CO₂ exchange of a boreal fen under contrasting WTD conditions i.e. shallow vs. deep WTD.~~ A May-October WTD drawdown of ~0.25 m from 2004 to 2009 hastened oxygen transport to microbial and root surfaces, enabling greater microbial and root energy yields, and peat and litter decomposition, which raised modelled ecosystem respiration (R_e) by $-0.26 \mu\text{mol CO}_2 \text{ m}^{-2} \text{ s}^{-1}$ per 0.1 m of WTD drawdown. It also augmented nutrient mineralization, and hence root nutrient availability and uptake, which resulted in improved leaf nutrient (nitrogen) status that facilitated carboxylation, and raised modelled vascular gross

85 primary productivity (GPP) and plant growth. The increase in modelled vascular GPP exceeded
 86 declines in modelled non-vascular (moss) GPP due to greater shading from increased vascular
 87 plant growth, and moss drying from near surface peat desiccation, thereby causing a net increase
 88 in modelled growing season GPP by $-0.39 \mu\text{mol CO}_2 \text{ m}^{-2} \text{ s}^{-1}$ per 0.1 m of WTD drawdown.
 89 Similar increases in GPP and R_e left no significant WTD effects on modelled seasonal and
 90 interannual variations in net ecosystem productivity (NEP). These modelled trends were
 91 corroborated well by eddy covariance measured hourly net CO_2 fluxes (modelled vs. measured:
 92 $R^2 \sim 0.8$, slopes $\sim 1 \pm 0.1$, intercepts $\sim 0.05 \mu\text{mol m}^{-2} \text{ s}^{-1}$), hourly measured automated chamber net
 93 CO_2 fluxes (modelled vs. measured: $R^2 \sim 0.7$, slopes $\sim 1 \pm 0.1$, intercepts $\sim 0.4 \mu\text{mol m}^{-2} \text{ s}^{-1}$), and
 94 other biometric and laboratory measurements. Modelled drainage as an analog for WTD
 95 drawdown induced by climate change driven drying showed that this boreal peatland would
 96 switch from a large carbon sink (NEP $\sim 160 \text{ g C m}^{-2} \text{ yr}^{-1}$) to carbon neutrality (NEP $\sim 10 \text{ g C m}^{-2}$
 97 yr^{-1}) should water table deepened by a further $\sim 0.5 \text{ m}$. This decline in projected NEP indicated
 98 that a further WTD drawdown at this fen would eventually lead to a decline in GPP due to water
 99 limitation. Therefore, representing the effects of interactions among hydrology, biogeochemistry
 100 and plant physiological ecology on ecosystem carbon, water, and nutrient cycling in global
 101 carbon models would improve our predictive capacity for changes in boreal peatland carbon
 102 sequestration under changing climates.

1. Introduction

Northern boreal peatlands have been accumulating carbon (C) at a rate of about 20-30 g m⁻² yr⁻¹ over several thousand years (Gorham, 1991; Turunen et al., 2002). Drier and warmer future climates can affect the resilience of long-term boreal peatland C stocks by lowering water table (WT) that can halt or even reverse the C accumulation in boreal peatlands (Limpens et al., 2008; Dise, 2009; Frolking et al., 2011). To maintain and protect the C sequestration potentials of boreal peatlands we need an improved predictive capacity of how these C stocks would behave under future drier and warmer climates. However, boreal peatland C processes are currently under-represented in global C models largely due to inadequate simulation of hydrologic feedbacks to C cycles (St-Hilaire et al., 2010; Sulman et al., 2012). This can be overcome by integrating interactions between eco-hydrology of peatland vegetation, and peat biogeochemistry into finer resolution process models that can eventually be scaled up into larger spatial and temporal scale C models (Waddington et al., 2015).

The hydrologic feedbacks to boreal peatland C processes are largely mediated by water table depth (WTD) variation and its effects on peat-microbe-plant-atmosphere exchanges of C, energy, water and nutrients (Grant et al., 2012). WTD drawdown can affect net ecosystem productivity (NEP) of boreal peatlands through its effects on ecosystem respiration (R_e) and gross primary productivity (GPP). Receding WT can cause peat pore drainage that enhances microbial O₂ availability, energy yields, growth and decomposition and hence increases R_e (Sulman et al., 2009, 2010; Cai et al., 2010; Flanagan and Syed, 2011; Peichl et al., 2014). The rate of increase in R_e due to the WTD drawdown may vary with peat moisture retention and quality of peat forming substrates (Preston et al., 2012). For instance, peats with low moisture retention exhibit more rapid pore drainage than those with high moisture retention thus causing

126 more increase in R_e for similar WTD drawdowns (Parmentier et al., 2009; Sulman et al., 2009,
127 2010; Cai et al., 2010). Peats formed from *Sphagnum* mosses degrade at rates slower than those
128 formed from remains of vascular plants (Moore and Basiliko, 2006). So for similar WTD
129 drawdowns, moss peats would generate less increase in microbial decomposition and hence R_e
130 than would sedge, reed or woody peats (Updegraff et al., 1995). Continued WTD drawdown can
131 also cause near surface peat desiccation from inadequate recharge through capillary rise from
132 deeper WT. Desiccation of near surface or shallow peat layers can cause a reduction in microbial
133 decomposition that can partially or fully offset the increased decomposition in the deeper peat
134 layers thereby yielding indistinct net effects of WTD drawdown on R_e (Dimitrov et al., 2010a).

135 The interactions between WTD and GPP vary across peatlands depending upon peat
136 forming vegetation. For instance, increased aeration due to WTD drawdown enhances root O_2
137 availability and growth in vascular plants (Lieffers and Rothwell, 1987; Murphy et al., 2009).
138 Enhanced root growth is also associated with greater root nutrient availability and uptake from
139 more rapid mineralization facilitated by greater microbial energy yields, growth and
140 decomposition under deeper WT (Choi et al., 2007). Greater root nutrient uptake in turns
141 increases the rate of vascular CO_2 fixation and hence GPP (Sulman et al., 2009, 2010; Cai et al.,
142 2010; Flanagan and Syed, 2011; Peichl et al., 2014). WTD drawdown, however, does not affect
143 the non-vascular (e.g., moss) GPP in the same way it does the vascular GPP (Lafleur et al.,
144 2005). Non-vascular plants mostly depend upon the water available for uptake in the near surface
145 or shallow peat layers (Dimitrov et al., 2011). These layers can drain quickly with receding WT
146 and thus have to depend on moisture supply through capillary rise from deeper WT (Dimitrov et
147 al., 2011; Peichl et al., 2014). If recharge through the capillary rise is not adequate, near surface
148 peat desiccation occurs which slows moss water uptake, causes eventual drying of mosses and

149 reduces moss GPP (Lafleur et al., 2005; Riutta 2008; Sonnentag et al., 2010; Sulman et al., 2010;
150 Dimitrov et al., 2011; Kuiper et al., 2014; Peichl et al., 2014). Near surface peat desiccation also
151 suppresses vascular root water uptake from the desiccated layers (Lafleur et al., 2005; Dimitrov
152 et al., 2011). But enhanced root growth and elongation facilitated by improved O₂ status in the
153 newly aerated deeper peat layers under deeper WT enables vascular roots to take up water from
154 wetter deeper layers (Dimitrov et al., 2011). If deeper root water uptake offsets the reduction in
155 water uptake from desiccated near surface layers, vascular transpiration (T), canopy stomatal
156 conductance (g_c) and hence GPP are sustained under deeper WT (Dimitrov et al., 2011). But if
157 the WT falls below certain threshold level under which deeper root water uptake can no longer
158 sustain vascular T , g_c and hence vascular GPP declines (Lafleur et al., 2005; Wu et al., 2010).

159 WTD variation can thus affect boreal peatland NEP through its effects on peat moisture
160 and aeration and consequent root and microbial oxidation-reduction reactions and energy yields.
161 To predict how boreal peatlands would behave under future drier and warmer climates, a
162 peatland C model thus needs to simulate WTD dynamics that determine the boundary between
163 aerobic and anaerobic zones and controls peat biogeochemistry. However, most of the current
164 process-based peatland C models either do not simulate a continuous anaerobic zone below a
165 prognostic WT (e.g., Baker et al., 2008; Schaefer et al., 2008; Tian et al., 2010), or do not
166 simulate peat saturation since any water in excess of field capacity is drained in those models
167 (e.g., Gerten et al., 2004; Krinner et al., 2005; Weng and Luo, 2008). Moreover, instead of
168 explicitly simulating the above-described hydrological and biological interactions between peat
169 aeration and biogeochemistry, most of those models use scalar functions of soil moisture
170 contents to inhibit R_e and GPP under low or high moisture conditions (e.g., Frohking et al., 2002;
171 Zhang et al., 2002; Bond-Lamberty et al., 2007; St-Hilaire et al., 2010; Sulman et al., 2012).

Consequently, those peatland C models could not simulate declines in GPP and R_e due to shallow WT while simulating WTD effects on CO₂ exchange of peatlands across northern US and Canada (Sulman et al., 2012). Furthermore, the approach of using scalar functions to simulate moisture limitations to GPP and R_e requires site-specific parameterization of model algorithms which reduces scalability of those peatland C models.

1.1. Objective and rationale

In this study, we tested a process-based ~~terrestrial~~-ecosystem model *ecosys* against eddy covariance (EC) net CO₂ fluxes measured over a drying period from 2004 to 2009 in a western Canadian boreal fen peatland in Alberta, Canada (will be termed as WPL hereafter) (Syed et al., 2006; Flanagan and Syed, 2011). The objective was to test whether the coupling of a dynamic WTD that arises from vertical and lateral water fluxes as a function of a soil moisture retention scheme with 1) oxygen transport, 2) microbial and root oxidation-reduction reactions and energy yields, and 3) root, microbial and plant growth and uptake within a soil-plant-microbe-atmosphere water, C and nutrient (nitrogen, phosphorus) scheme in an ecosystem process model could explain underlying processes that govern hydrological effects on net CO₂ exchange of a northern boreal fen under contrasting WTD conditions (e.g., shallower vs. deeper WTD). This study would reconcile our knowledge on the feedback mechanisms among hydrology, eco-physiology, and biogeochemistry of peatlands which are predominantly based upon inferences drawn from EC-gap filled values that include empirically modelled estimates. It would also provide us with a better ~~insight~~insight into- and an improved predictive capacity ~~of~~on how carbon deposits in northern boreal peatlands would behave under changing climates. Rigorous site-scale testing of coupled eco-hydrology and biogeochemistry algorithms in ecosystem

process models such as *ecosys* would also provide us with important insights ~~to-on how to~~ improve large-scale representation of these processes into next generation land surface models.

1.2. Hypotheses

In an eddy covariance (EC) study, Flanagan and Syed (2011) found no net effect of a weather driven WTD drawdown on NEP of WPL over 2004–2009. From the regressions of EC-derived GPP and R_e on site measured WTD, they inferred that the absence of a net WTD effect on NEP was caused by similar increases in GPP and R_e with WTD drawdown. We hypothesized that coupled eco-hydrology and biogeochemistry algorithms in *ecosys* would be able to simulate and explain underlying mechanisms of these effects of WTD drawdown on GPP and R_e and hence NEP at the WPL. We tested the following four central hypotheses:

(1) WTD drawdown would increase R_e of the northern fen at the WPL. This effect of WTD drawdown on R_e ~~could-would~~ be modelled by simulation of peat pore drainage and improved peat aeration that would increase the energy yields from aerobic microbial decomposition and hence would increase R_e .

(2) WTD drawdown would increase GPP of the northern fen at the WPL. This effect of WTD drawdown on GPP ~~could-would~~ be modelled by simulating enhanced microbial activity due to WTD drawdown that would cause more rapid nutrient mineralization and greater root nutrient availability and uptake, greater leaf nutrient concentrations and hence increased GPP.

(3) Increase in R_e with WTD drawdown (hypothesis 1) would cease should WTD ~~fall-fall~~ below a threshold depth. This threshold WTD effect on R_e ~~would~~ be modelled by simulating inadequate recharge of the near surface peat layers through capillary rise from the deeper WTD below the threshold level that would cause desiccation of those layers. Drying of near surface

peat layers and the surface residue ~~w~~eould reduce near surface and surface peat respiration that would partially offset the increase in deeper peat respiration due to aeration.

(4) Net effect of threshold WTD on GPP would be driven by the balance between how WTD would affect vascular vs. non-vascular GPP. This threshold WTD effect on GPP would be modelled by simulating vascular vs. non-vascular water relations under deeper WTD below the threshold level. Near surface peat desiccation in hypothesis 3 would reduce peat water potential and hydraulic conductivity and hence vascular and non-vascular water uptake from desiccated near surface layers. Since non-vascular mosses depend mainly on near surface peat layers for moisture supply, reduction in moss water uptake would cause a reduction in moss water potential and hence moss GPP. On the contrary, suppression of vascular root water uptake from desiccated near surface layers under deeper WT would be offset by increased deeper root water uptake from newly aerated deeper peat layers with higher water potentials that would sustain vascular canopy water potential (ψ_c), canopy stomatal conductance (g_c) and GPP.

2. Methods

2.1. Model development

Ecosys is a process-based ~~terrestrial~~-ecosystem model ~~that-which~~ simulates 3D water, energy, carbon and nutrient (nitrogen, phosphorus) cycles in different peatlands (Dimitrov et al., 2011; Grant et al., 2012; Sulman et al., 2012; Mezbahuddin et al., 2014, 2015, 2016). *Ecosys* algorithms that govern the modelled effects of WTD variations on ~~ecosystem-peatland~~ net CO₂ exchange ~~which-are-related-to-our-hypotheses~~ are described below. These algorithms in *ecosys* ~~a~~are derived from published independent basic research which describe eco-hydrological and biogeochemical mechanisms that govern carbon, nutrient (N, P), water, and energy balance of a typical boreal peatland ecosystem (Fig. 1)~~terrestrial-ecosystems. Equations representing e~~*Ecosys*

algorithms which are related to our hypotheses are depicted as a flowchart (Fig. 1) and cited as
equations within the text. These equations are, and are also listed in ~~the~~ sections S1-S4 ~~in of~~ the
supplementary material with references to their sources for further clarification. These site-
independent basic ~~terrestrial~~-ecosystem process algorithms in *ecosys* are thus not parameterized
for each peatland site. Instead the coupled algorithms are fed with peatland-specific measurable
soil, weather, vegetation and management inputs to simulate C, nutrient (N, P), water and energy
balance of ~~that a~~ particular peatland ecosystem.

2.1.1. Water table depth (WTD)

The WTD in *ecosys* is calculated at the end of each time step as the depth to the top of the
saturated zone below which air-filled porosity is zero (Eq. D32). It is the depth at which lateral
water flux is in equilibrium with the difference between vertical influxes (precipitation) and
effluxes (evapotranspiration). Lateral water transfer between modelled grid cells in *ecosys* and
the adjacent ecosystem occurs to and from a set external WTD (WTD_x) over a set distance (L_t)
(Fig. 2). The WTD_x represents average watershed WTD with reference to average hummock
surface. The WTD in *ecosys* is thus not prescribed, but rather controls, and is controlled by
lateral and vertical surface and subsurface water fluxes (Eqs. D1-D31). More detail about how
peatland WTD, vertical and lateral soil water flow, and soil moisture retention are modelled in
ecosys can be found in Dimitrov et al. (2010b) and Mezbahuddin et al. (2015, 2016).

2.1.2. Heterotrophic respiration and WTD

WTD fluctuation in *ecosys* determines the boundary between and the extent of aerobic vs.
anaerobic soil zones. So WTD fluctuation affects *ecosys*'s algorithms of organic oxidation-
reduction transformations and microbial energy yields, which drive microbial growth, substrate
decomposition and uptake (Fig. 1) (Eqs. A1-A30). Organic transformations in *ecosys* occur in a

262 residue layer and in each of the user defined soil layers within five organic matter-microbe
 263 complexes i.e., coarse woody litter, fine non-woody litter, animal manure, particulate organic C
 264 and humus (Fig. 1). Each of the complexes has three decomposition substrates i.e., solid organic
 265 C, sorbed organic C and microbial residue C; the decomposition agent i.e., microbial biomass;
 266 and the decomposition product i.e., dissolved organic C (DOC) (Fig. 1). Rates of the
 267 decomposition and resulting DOC production in each of the complexes is a first-order function
 268 of the fraction of substrate colonized by active biomasses (M) of diverse microbial functional
 269 types (MFTs). The MFTs in *ecosys* are obligate aerobes (bacteria and fungi), facultative
 270 anaerobes (denitrifiers), obligate anaerobes (fermenters), heterotrophic (acetotrophic) and
 271 autotrophic (hydrogenotrophic) methanogens, and aerobic and anaerobic heterotrophic
 272 diazotrophs (non-symbiotic N_2 fixers) (Fig. 1) (Eqs. A1-A2, A4). Biomass (M) growth of each of
 273 the MFTs (Eq. A25a) is calculated from its DOC uptake (Fig. 1) (Eq. A21). The rate of M
 274 growth is driven by energy yield from growth respiration (R_g) (Eq. A20) that is calculated by
 275 subtracting maintenance respiration (R_m) (Eq. A18) from heterotrophic respiration (R_h) (Eq.
 276 A11). The values of R_h are driven by oxidation of DOC (Eq. A13). DOC oxidation may be
 277 limited by microbial O_2 reduction (Eq. A14) driven by microbial O_2 demand (Eq. A16) and
 278 constrained by O_2 diffusion calculated from aqueous O_2 concentrations in soil ($[O_{2s}]$) (Eq. A17).
 279 Values of $[O_{2s}]$ are maintained by convective-dispersive transport of O_2 from the atmosphere to
 280 gaseous and aqueous phases of the soil surface layer (Eq. D41), by convective-dispersive
 281 transport of O_2 through gaseous and aqueous phases in adjacent soil layers (Eqs. D42, D44), and
 282 by dissolution of O_2 from gaseous to aqueous phases within each soil layer (Eq. D39).
 283 Shallow WTD in *ecosys* can cause lower air-filled porosity (θ_g) in the wetter peat layers
 284 above the WT. Lower θ_g reduces O_2 diffusivity in the gaseous phase (D_g) (Eq. D44) and gaseous

285 O₂ transport (Eqs. D41-D42) in these layers. Peat layers below the WT have zero θ_g that prevents
 286 gaseous O₂ transport in these layers. So, under shallow WT, [O_{2s}] relies more on O₂ transport
 287 through the slower aqueous phase (Eq. D42) which causes a decline in [O_{2s}]. Decline in [O_{2s}]
 288 slows O₂ uptake (Eq. A17) and hence R_h (Eq. A14), R_g (Eq. A20) and growth of M (Eq. A25).
 289 Lower M slows decomposition of organic C (Eqs. A1-A2) and production of DOC which further
 290 slows R_h (Eq. A13), R_g and growth of M (Fig. 1). Although some MFTs can sustain DOC
 291 oxidation by reducing alternative electron acceptors (e.g., methanogens reducing acetate or CO₂
 292 to CH₄, and denitrifiers reducing NO_x to N₂O or N₂), lower energy yields from these reactions
 293 reduce R_g (Eq. A21), and hence M growth, organic C decomposition and subsequent DOC
 294 production (Fig. 1). Slower decomposition of organic C under low [O_{2s}] also causes slower
 295 decomposition of organic nitrogen (N) and phosphorus (P) (Eq. A7) and production of dissolved
 296 organic nitrogen (DON) and phosphorus (DOP), which causes slower uptake of microbial N and
 297 P (Eq. A22) and growth of M (Eq. A29) (Fig. 1). Slower M growth causes slower mineralization
 298 (Eq. A26), and hence lowers aqueous concentrations of NH₄⁺, NO₃⁻ and H₂PO₄⁻ (Fig. 1).

299 WTD drawdown can increase θ_g that results in greater D_g (Eq. D44) and more rapid
 300 gaseous O₂ transport. A consequent rise in [O_{2s}] increases O₂ uptake (Eq. A17) and R_h (Eq. A14),
 301 R_g (Eq. A20) and growth of M (Eq. A25). Larger M hastens decomposition of organic C (Eqs.
 302 A1-A2) and production of DOC which further hastens R_h (Eq. A13), R_g and growth of M . More
 303 rapid decomposition of organic C under adequate [O_{2s}] in this period also causes more rapid
 304 decomposition of organic N and P (Eq. A7) and production of DON and DOP, which increases
 305 uptake of microbial N and P (Eq. A22) and growth of M (Eq. A29) (Fig. 1). Rapid M growth
 306 causes rapid mineralization (Eq. A26), and hence greater aqueous concentrations of NH₄⁺, NO₃⁻
 307 and H₂PO₄⁻ (Fig. 1).

When WTD recedes below a certain threshold level, capillary rise from the WT can no longer support adequate recharge of the near surface peat layers and the surface litter (Eqs. D9, D12). It causes desiccation of the residue and the near surface peat layers thereby causing a reduction in water potential (ψ_s) and an increase in aqueous microbial concentrations ($[M]$) in each of these layers (Eq. A15). Increased $[M]$ caused by the peat desiccation reduces microbial access to the substrate for decomposition in each of the desiccated layers and reduces R_h (Eq. A13). Reduction in R_h is calculated in *ecosys* from competitive inhibition of microbial exoenzymes with increasing concentrations (Eq. A4) (Lizama and Suzuki, 1991).

2.1.3. WTD effects on vascular gross primary productivity

Ecosys simulates effects of WTD variation on vascular GPP from WTD variation effects on root O_2 and nutrient availability and root growth and uptake. Root O_2 and nutrient uptake in *ecosys* are coupled with a hydraulically driven soil-plant-atmosphere water scheme. Root growth in each vascular plant population in *ecosys* is calculated from its assimilation of the non-structural C product of CO_2 fixation (σ_c) (Eq. C20). Assimilation is driven by R_g (Eq. C17) remaining after subtracting R_m (Eq. C16) from autotrophic respiration (R_a) (Eq. C13) driven by oxidation of σ_c (Eq. C14). Oxidation in roots may be limited by root O_2 reduction (Eq. C14b) which is driven by root O_2 demand to sustain C oxidation and nutrient uptake (Eq. C14e), and constrained by O_2 uptake controlled by concentrations of aqueous O_2 in the soil ($[O_{2s}]$) and roots ($[O_{2r}]$) (Eq. C14d). Values of $[O_{2s}]$ and $[O_{2r}]$ are maintained by convective-dispersive transport of O_2 through soil gaseous and aqueous phases and root gaseous phase (aerenchyma) respectively and by dissolution of O_2 from soil and root gaseous to aqueous phases (Eqs. D39-D45). O_2 transport through root aerenchyma depends on species-specific values used for root air-filled porosity (θ_{pr}) (Eq. D45). Shallow WTD and resultant high peat moisture content in *ecosys*

331 can cause low θ_g that reduces soil O_2 transport, forcing root O_2 uptake to rely more on $[O_{2r}]$ and
 332 hence on root O_2 transport determined by θ_{pr} . If this transport is inadequate, decline in $[O_{2r}]$
 333 slows root O_2 uptake (Eqs. C14c-d) and hence R_a (Eq. C14b), R_g (Eq. C17) and root growth (Eq.
 334 C20b) and root N and P uptake (Eqs. C23b, d, f) (Fig. 1). Root N and P uptake under shallow
 335 WT is further slowed by reductions in aqueous concentrations of NH_4^+ , NO_3^- and $H_2PO_4^-$ (Eqs.
 336 C23a, c, e) from slower mineralization of organic N and P (Fig. 1). Slower root N and P uptake
 337 reduces concentrations of non-structural N and P products of root uptake (σ_N and σ_P) with
 338 respect to that of σ_C in leaves (Eq. C11), thereby slowing CO_2 fixation (Eq. C6) and GPP.

339 WTD drawdown facilitates rapid D_g which allows root O_2 demand to be almost entirely
 340 met from $[O_{2s}]$ (Eqs. C14c-d) and so enables more rapid root growth and N and P uptake (Eqs.
 341 C23b, d, f). Increased root growth and nutrient uptake is further stimulated by increased aqueous
 342 concentrations of NH_4^+ , NO_3^- and $H_2PO_4^-$ (Eqs. C23a, c, e) from more rapid mineralization of
 343 organic N and P during deeper WT (Fig. 1). Greater root N and P uptake increases
 344 concentrations of σ_N and σ_P with respect to σ_C in leaves (Eq. C11), thereby facilitating rapid CO_2
 345 fixation (Eq. C6) and GPP. When WT falls below a certain threshold, inadequate capillary rise
 346 (Eqs. A9, A12) from deeper WT causes near-surface peat desiccation that reduces soil water
 347 potential (ψ_s) and raises soil hydraulic resistance (Ω_s) (Eq. B9), thereby forcing lower root water
 348 uptake (U_w) from desiccated layers (Fig. 1) (Eq. B6). However, deeper rooting facilitated by
 349 increased $[O_{2s}]$ under deeper WT can sustain U_w (Eq. B6) from wetter deeper peat layers with
 350 higher ψ_s and lower Ω_s (Eq. B9). If U_w from the deeper wetter layers cannot offset the
 351 suppression in U_w from desiccated near surface layers, the resultant net decrease in U_w causes a
 352 reduction in root, canopy and turgor potentials (ψ_r , ψ_c and ψ_n) (Eq. B4) and hence g_c (Eq. B2b) in

353 *ecosys* when equilibrating U_w with transpiration (T) (Eq. B14). Lower g_c reduces CO_2 diffusion
354 into the leaves thereby reducing CO_2 fixation (Eq. C6) and GPP (Eq. C1) (Fig. 1).

355 **2.1.4. WTD effects on non-vascular gross primary productivity**

356 *Ecosys* simulates non-vascular plants (e.g., mosses) as tiny plants with no stomatal
357 regulations that grow on modelled hummock and hollow grid cells (Dimitrov et al., 2011).
358 Model input for moss population is usually larger and hence intra-specific competition for lights
359 and nutrients is greater so that individual moss plant and moss belowground growth (i.e. root like
360 structures for water and nutrient uptake) are smaller (Eq. C21b). Shallower belowground growth
361 of simulated mosses in *ecosys* means the water uptake of mosses are mostly confined to the near
362 surface peat layers. When WT deepens past a threshold level, inadequate capillary rise (Eqs. D9,
363 D12) causes near-surface peat desiccation, thereby reducing ψ_s and increasing Ω_s (Eq. B9) of
364 those layers (Fig. 1). It causes a reduction in moss canopy water potential (ψ_c) while
365 equilibrating moss evaporation with moss U_w (Eq. B6). Reduced moss ψ_c causes a reduction in
366 moss carboxylation rate (Eqs. C3, C6a) and moss GPP (Fig. 1) (Eq. C1).

367 **2.2. Modelling experiment**

368 **2.2.1. Study site**

369 The peatland eco-hydrology and biogeochemistry algorithms in *ecosys* were tested in this
370 study against measurements of WTD and ecosystem net CO_2 fluxes at a flux station of the
371 Fluxnet-Canada Research Network established at the WPL (latitude: 54.95°N, longitude:
372 112.47°W). The study site is a moderately nutrient-rich treed fen peatland within the Central
373 Mixed-wood Sub-region of Boreal Alberta, Canada. Peat depth around the flux station was about
374 2 m. This peatland is dominated by stunted trees of black spruce (*Picea mariana*) and tamarack
375 (*Larix laricina*) with an average canopy height of 3 m. High abundance of a shrub species *Betula*

376 *pumila* (dwarf birch), and the presence of a wide range of mosses e.g., *Sphagnum* spp., feather
377 moss, and brown moss characterize the under-storey vegetation of WPL. The topographic,
378 climatic, edaphic and vegetative characteristics of this site were described in more details by
379 Syed et al. (2006).

380 2.2.2. Field data sets

381 *Ecosys* model inputs of half hourly weather variables i.e. incoming shortwave and
382 longwave radiation, air temperature (T_a), wind speed, precipitation and relative humidity during
383 2003-2009 were measured by Syed et al. (2006) and Flanagan and Syed (2011) at the
384 micrometeorological station installed at the WPL. To test the adequacy of WTD simulation in
385 *ecosys*, modelled outputs of hourly WTD were tested against WTD measured at the WPL with
386 respect to average hummock surface by Flanagan and Syed (2011). To examine how well *ecosys*
387 simulated net ecosystem CO₂ exchange at the WPL, we tested hourly modelled net ecosystem
388 CO₂ fluxes against hourly ~~accumulated~~ averaged measurements (average of two half-hourly)
389 collected by Syed et al. (2006) and Flanagan and Syed (2011) by using eddy covariance (EC)
390 micro-meteorological approach. Each of these EC-measured net CO₂ fluxes consisted of an eddy
391 flux and a storage flux (Syed et al. 2006). Erroneous flux measurements due to stable air
392 conditions were screened out with the use of a minimum friction velocity (u^*) threshold of 0.15
393 m s⁻¹ (Syed et al. 2006). The net CO₂ fluxes that survived the quality control were used to derive
394 half hourly R_e (=nighttime net CO₂ fluxes) and GPP (=daytime net CO₂ fluxes – R_e) (Barr et al.,
395 2004; Syed et al., 2006). To derive daily, seasonal and annual estimates of GPP, and R_e , the data
396 gaps resulting from the quality control were filled based on empirical relationships between soil
397 temperature at a shallow depth (0.05 m) and measured half hourly R_e , and between incoming
398 shortwave radiation and measured half hourly GPP using 15-days moving windows. The gap-

399 filled R_e and GPP were then summed up for each half hour to fill NEP data gaps to derive daily,
400 seasonal and annual estimates of EC-gap filled NEP (Barr et al., 2004; Syed et al., 2006).

401 Soil CO₂ fluxes measured by automated chambers can provide a valuable supplement to
402 EC CO₂ fluxes in testing modelled respiration by providing more continuous measurements than
403 EC. So, we ~~also~~ tested our modelled outputs against half-hourly automated chamber
404 measurements by Cai et al. (2010) at the WPL. These CO₂ flux measurements were carried out
405 during ice-free periods (May-October) of 2005 and 2006 over both hummocks and hollows by
406 using a total of 9 non-steady state automatic transparent chambers (Cai et al., 2010). Along with
407 soil respiration these chamber CO₂ fluxes included fixation and autotrophic respiration from
408 dwarf shrubs, herbs and mosses (Cai et al., 2010).

409 Modelled WTD effects on peatland biogeochemistry and hence on peatland nutrient and
410 carbon cycling were also corroborated against leaf nitrogen concentrations, foliar N to P ratios, N
411 mineralization, and rooting depths biometrically measured at either our site or at sites that had
412 similar peat substrates, hydrology and/or plant functional types. Needles of black spruce and
413 tamarack, and leaves of dwarf birch were sampled over our study site during mid-summer of
414 2004 for foliar nutrient content analyses (Syed et al., 2006). Leaf nitrogen contents were
415 analyzed on N₂ gas that were generated from reduction of dried leaf tissues in an elemental
416 analyzer and quantified using a gas isotope ratio mass spectrometer (Syed et al., 2006). Leaf
417 phosphorus contents were analyzed on black spruce and tamarack needle leaf tissues that were
418 dry-ashed and then digested using a dilute HNO₃ and HCl mixture and then quantified using an
419 Inductively Coupled Plasma (ICP) spectroscopic analysis technique (Syed et al., 2006).

Formatted: Subscript

Formatted: Subscript

2.2.3. Model run

Ecosys model run to simulate WTD effects on net CO₂ exchange of WPL had a hummock and a hollow grid cell that exchanged water, heat, carbon and nutrients (N, P) between them and with surrounding vertical and lateral boundaries (Fig. 2). The hollow grid cell had near surface peat layer that was 0.3 m thinner than the hummock cell representing a hummock-hollow surface difference of 0.3 m observed in the field (Long, 2008) (Fig. 2). Any depth with respect to the modelled hollow surface would thus be 0.3 m shallower than the depth with respect to the modelled hummock surface.

Peat organic and chemical properties at different depths of the WPL were represented in *ecosys* by inputs from measurements either at the site (e.g., Syed et al., 2006; Flanagan and Syed, 2011) or at similar nearby sites (e.g., Rippey and Nelson, 2007) (Fig. 2). *Ecosys* was run for a spin up period of 1961-2002 under repeating 7-year sequences of hourly weather data (shortwave and longwave radiation, air temperature, wind speed, humidity and precipitation) recorded at the site from 2003 to 2009. There was a drying trend observed from 2003 to 2009 due to diminishing precipitation that caused WTD drawdown in the watershed in which WPL is located, which lowered the WT of this fen peatland (Flanagan and Syed, 2011). To accommodate the gradual drying effects of catchment hydrology on modelled fen peatland WTD, we set the WTD_x at different levels based on the annual wetness of weather, e.g., shallow, intermediate, and deep (WTD_x=0.19, 0.35 and 0.72 m below the hummock surface, or 0.11 m above and 0.05 and 0.42 m below the hollow surface) (Fig. 2). There was no exchange of water through lower model boundary to represent the presence of nearly impermeable clay sediment underlying the peat (Syed et al., 2006) (Fig. 2). Variations in peat surface with WTD variations, which is an

important hydrologic self-regulation of boreal peatlands (Dise, 2009), was not represented in this version of *ecosys*.

At the start of the spin up run, the hummock grid cell was seeded with an evergreen needle leaf and a deciduous needle leaf over-storey plant functional types (PFT) to represent the black spruce and tamarack trees at the WPL. The hollow grid cell was seeded with only the deciduous needle leaf over-storey PFTs since the black spruce trees at the WPL only grew on the raised areas. Each of the modelled hummock and the hollow was also seeded with a deciduous broadleaved vascular (to represent dwarf birch) and a non-vascular (to represent mosses) under-storey PFTs. The planting densities were such that the population densities of the black spruce, tamarack, dwarf birch and moss PFTs were 0.16, 0.14, 0.3, and 500 m⁻² respectively at the end of the spin up run so as to best represent field vegetation (Syed et al., 2006; Mezbahuddin et al., 2016). To include wetland adaptation, we used a root porosity (θ_{pr}) value of 0.1 for the two over-storey PFTs and a higher θ_{pr} value of 0.3 for the under-storey vascular PFT to represent better wetland adaptation in the under-storey than the over-storey PFTs. These θ_{pr} values were used in calculating root O₂ transport through aerenchyma (Eq. D45) and did not change with waterlogging throughout the model run. These θ_{pr} values were representatives of root porosities measured for various northern boreal peatland plant species (Cronk and Fennessy, 2001). Non-symbiotic N₂ fixation through association of cyanobacteria and mosses are also reported for Canadian boreal forests (Markham, 2009). This was represented in *ecosys* as N₂ fixation by non-symbiotic heterotrophic diazotrophs (Eq. A27) in the moss canopy. Further details about *ecosys* model set up to represent the hydrological, physical and ecological characteristics of WPL can be found in Mezbahuddin et al. (2016).

464 When the modelled ecosystem attained stable values of net ecosystem CO₂ exchange at
465 the end of the spin-up run, we continued the spin up run into a simulation run from 2003 to 2009
466 by using a real-time weather sequence. We tested our outputs from 2004-2009 of the simulation
467 run against the available site measurements of WTD, net EC CO₂ fluxes and net chamber CO₂
468 fluxes over those years.

469 **2.2.4. Model validation**

470 To examine the adequacy of modelling WTD effects on canopy, root and soil CO₂ fluxes
471 which were summed for net ecosystem CO₂ exchange at the WPL, we spatially averaged hourly
472 net CO₂ fluxes modelled over the hummock and the hollow to represent a 50:50 hummock-
473 hollow ratio and then regressed against hourly EC measured net ecosystem CO₂ fluxes for each
474 year from 2004-2009 with varying WTD. Each of these hourly EC measured net ecosystem CO₂
475 fluxes used in these regressions is an average of two half-hourly net CO₂ fluxes measured at a
476 friction velocity (u^*) greater than 0.15 m s⁻¹ that survived quality control procedure (Sec. 2.2.2).
477 Model performance was evaluated from regression intercepts ($a \rightarrow 0$), slopes ($b \rightarrow 1$), coefficients
478 of determination ($R^2 \rightarrow 1$), and root means squares for errors (RMSE $\rightarrow 0$) for each study year to
479 test whether there was any systematic divergence between the modelled and EC measured CO₂
480 fluxes.

481 Similar regressions were performed between modelled and automated chamber measured
482 net CO₂ fluxes for ice free periods (May-October) of 2005 and 2006 to further test the robustness
483 of modelled soil respiration under contrasting WTD conditions. Each of the half-hourly
484 measured chamber net CO₂ fluxes included soil respiration, and fixation and autotrophic
485 respiration from understorey vegetation (e.g., shrubs, herbs and mosses). So, we combined
486 modelled soil respiration with modelled fixation and autotrophic respiration from understorey

PFTs for comparison against these chamber measured net CO₂ fluxes. We also averaged net CO₂ flux measurements from all of the 9 chambers for each half hour to accommodate the variations in those fluxes due to microtopography (e.g., hummock vs. hollow). Two half hourly averaged values of net CO₂ fluxes were then averaged again to get hourly mean net chamber CO₂ fluxes for comparison against modelled hourly sums of soil and understorey fluxes averaged over modelled hummock and hollow. Model performance was evaluated from regression intercepts ($a \rightarrow 0$), slopes ($b \rightarrow 1$), coefficients of determination ($R^2 \rightarrow 1$), and root means squares for errors (RMSE $\rightarrow 0$) for each of 2005 and 2006.

2.2.5. Sensitivity of modelled peatland CO₂ exchange to artificial drainage

Large areas of northern boreal peatlands in Canada have been drained primarily for increased forest and agricultural production since plant productivity in pristine peatlands are known to be constrained by shallow WTD (Choi et al., 2007). Drainage and resultant WTD drawdown can affect both GPP and R_e on a short-term basis and the vegetation composition on a longer time scale thereby changing overall net CO₂ exchange trajectories of a peatland. To predict short-term effects of drainage on WTD and hence ecosystem net CO₂ exchange of WPL, we extended our simulation run into a projection run consisting two 7-yr cycles by using repeated weather sequences of 2003-2009. While doing so, we forced a stepwise drawdown in WTD_x by 1.0 and 2.0 m from that used in spin-up and simulation runs (Fig. 2) in the first (drainage cycle 1) and the second cycle (drainage cycle 2) respectively. This projection run would give us a further insight about how the northern boreal peatland of Western Canada would be affected by further WTD drawdown as a result of drier and warmer weather as well as a disturbance such as drainage. It would also provide us with a test of how sensitive the modelled

C processes were to the changes in model lateral boundary condition as defined by WTD_x in *ecosys*.

3. Results

3.1. Model performance in simulating diurnal variations in ecosystem net CO₂ fluxes

Variations in precipitation can cause change in WTD and consequent variation in diurnal net CO₂ exchange across years. *Ecosys* simulated hourly EC-measured net CO₂ fluxes well over 2004-2008 with varying precipitation (Table 1a). On a year-to-year basis, regressions of hourly modelled vs. EC-measured net ecosystem CO₂ fluxes gave intercepts within 0.1 μmol m⁻² s⁻¹ of zero, and slopes within 0.1 of one, indicating minimal bias in modelled outputs during each year from 2004-2008 (Table 1a). On a growing season (May-August) basis, regressions of modelled on measured hourly net CO₂ fluxes yielded larger positive intercepts from 2004-2009 (Table 1b). The larger intercepts were predominantly caused by modelled overestimation of growing season day-time CO₂ fluxes. This overestimation was offset by modelled overestimation of night-time CO₂ fluxes during the winter thus yielding smaller intercepts from throughout-the-year regressions of modelled vs. EC measured fluxes (Tables 1a vs. b). Values for coefficients of determination (R^2) were ~ 0.8 ($P < 0.001$) for all years from both throughout-the-year and growing season regressions (Tables 1a, b). RMSEs were < 2.0 and ~2.5 μmol m⁻² s⁻¹ for whole year regressions from 2004-2008 (Table 1a) and for growing season regressions from 2004-2009 (Table 1b) respectively. Much of the variations in EC measured CO₂ fluxes that was not explained by the modelled fluxes could be attributed to a random error of ~20% in EC methodology (Wesely and Hart, 1985). This attribution was further corroborated by root mean squares for random errors (RMSRE) in EC measurements, calculated for forests with similar CO₂ fluxes from Richardson et al. (2006) that were similar to RMSE (Tables 1a, b). The similar

values of RMSE and RMSRE also indicated that further constraint in model testing could not be achieved without further precision in EC measurements.

Regressions of modelled vs. chamber measured net CO₂ fluxes gave R^2 of ~0.7 for ice-free periods (May-October) of 2005 and 2006 indicated that the variations in soil respiration, and the fixation and aboveground autotrophic respiration due to WTD drawdown were modelled well (Table 1c). Smaller intercepts from those regressions meant lower model biases in simulating soil and understorey CO₂ fluxes under deepening WT (Table 1c). Although the slope was within 0.1 of one in 2005, it was a bit smaller in 2006 indicating lower modelled vs. chamber measured soil and understorey net CO₂ fluxes in 2006 (Table 1c). It was because some of the nighttime chamber fluxes in warmer nights of summer 2006 were as large as the EC measured ecosystem net CO₂ fluxes corresponding to those same hours which could not be modelled to their full extent. RMSE lower than RMSRE meant the errors in modelling soil and understorey CO₂ fluxes were within the limit of random errors due to chamber measurements (Table 1c). It further indicated the robustness of modelled outputs for soil and understorey CO₂ fluxes under different WTD conditions (e.g., shallower in 2005 vs. deeper in 2006) (Table 1c).

3.2. Seasonality in WTD and net ecosystem CO₂ exchange

Ecosys simulated the seasonal and interannual variations in WTD from 2004 to 2009 well at the WPL (Figs. 3b, d, f, h, j, l) (Mezbahuddin et al., 2016). Seasonality in net CO₂ exchange at the WPL was predominantly governed by that in temperature which controlled the seasonality in phenology and GPP as well as that in R_e . *Ecosys* simulated the seasonality in phenology and hence GPP, and R_e well during a gradual growing season WTD drawdown from 2004 to 2009 which was apparent by good agreements between modelled vs. EC-gap filled daily NEP (Fig. 3) and modelled vs. EC-measured hourly net CO₂ fluxes (Table 1). Modelled NEP throughout the

winters of most of the years were more negative than the EC-gap filled NEP indicating larger modelled CO₂ effluxes than EC-gap filled fluxes during the winter (Fig. 3). The onset of photosynthesis at the WPL varied interannually depending upon spring temperature which was also modelled well by *ecosys*. For instance, *ecosys* modelled a smaller early growing season (May) GPP and hence NEP in 2004 with a cooler spring than 2005 which was also apparent in daily EC-gap filled NEP (Figs. 3a vs. c).

3.3. WTD effects on diurnal net ecosystem CO₂ exchange

WTD variation can affect diurnal net CO₂ exchange by affecting peat O₂ status and consequently root and microbial O₂ and nutrient availability, growth and uptake thereby influencing CO₂ fixation and respiration. *Ecosys* simulated WTD effects on diurnal net CO₂ exchange at the WPL well over three 10-day periods with comparable weather conditions (radiation and air temperature) during late growing seasons (August) of 2005, 2006 and 2008 (Fig. 4). A WTD drawdown from August 2005 to August 2006 in *ecosys* caused a reduction in peat water contents and a consequent increase in O₂ influxes from atmosphere into the peat that eventually caused an increase in modelled soil CO₂ effluxes (Fig. 5c). This stimulation of soil respiration was corroborated by modelled vs. chamber measured (Cai et al., 2010) night-time soil CO₂ fluxes and understorey autotrophic respiration (R_a) in August 2006 with deeper WTD which were larger than those in 2005 with shallower WTD (Fig. 5b). Larger modelled soil CO₂ effluxes in 2006 contributed to the larger modelled ecosystem CO₂ effluxes (R_e) that was also apparent in night-time EC CO₂ fluxes in 2006 which were larger than those in 2005 (Fig. 5a).

Continued WTD drawdown into the late growing season of 2008 (Fig. 4c) sustained improved peat oxygenation and hence larger modelled soil CO₂ effluxes (Fig. 5c). Consequently, modelled night-time net ecosystem CO₂ fluxes, and soil and understorey CO₂ fluxes in 2006 and

578 in 2008 were similarly larger than those in 2005 which was corroborated well by EC measured
579 night-time fluxes during 2006 and 2008 vs. 2005 (Figs. 5a-b). Although night-time modelled and
580 EC measured net ecosystem CO₂ fluxes in 2008 were larger than those in 2005, the day-time
581 modelled and EC measured CO₂ fluxes in 2008 did not decline with respect to those in 2005
582 (Fig. 5a). Similar day-time fluxes in 2005 and 2008 despite larger night-time fluxes in 2008 than
583 in 2005 indicated a greater late growing season CO₂ fixation in 2008 with deeper WTD than in
584 2005 with shallower WTD.

585 Beside WTD, temperature variation also profoundly affected ecosystem net CO₂
586 exchange at the WPL. For a given WTD condition warmer weather caused increases in R_e at the
587 WPL (Figs. 4b-c and 5a-b). Night-time modelled, and EC and chamber measured ecosystem,
588 soil, and understorey CO₂ fluxes, in warmer nights of day 214, 220 and 222 were larger than
589 those in cooler nights of day 221, 224 and 218 in 2005, 2006 and 2008 respectively (Figs. 4b and
590 ~~53~~5a-b). However, for a given temperature modelled and EC-gap filled night-time ecosystem CO₂
591 fluxes, and modelled and chamber measured night-time soil and understorey CO₂ fluxes were
592 larger under deeper WT conditions in 2006 and 2008 than under shallower WT condition in 2005
593 (denoted by the grey arrows in Figs. 4b and 5a-b). It showed net WTD drawdown effect on R_e
594 (separated from temperature effect) and hence on NEP.

595 The degree of R_e stimulation due to warming was also influenced by WTD at the WPL.
596 The warming events in early to mid-August of 2006 and 2008, when WT was deeper than in late
597 July of 2005, caused gradual increases in modelled, and EC and chamber measured night-time
598 ecosystem, soil and understorey CO₂ effluxes ($=R_e$) (Figs. 6h, i, k, l). This R_e stimulation due to
599 warming under deeper WT contributed to declines in modelled and EC-gap filled July-August
600 NEP in 2006 and 2008 (Figs. 3e, i). Lack of similar stimulation in R_e with warming under

shallower WT in 2005 did not yield a similarly evident stimulation of either modelled or EC or chamber measured ecosystem, soil and understorey night-time CO₂ effluxes (Figs. 6g, j vs. h, i, k, l) which resulted in the absence of decline in July-August NEP as occurred in 2006 and 2008 (Figs. 3c vs. e, i). Greater warming driven R_e stimulation under deeper WT further indicated the importance of WTD in mediating potential effects of future warmer climates on boreal peatland NEP.

3.4. Interannual variations in WTD and net ecosystem productivity

The effects of WTD drawdown on modelled and EC-gap filled diurnal net ecosystem CO₂ exchange also contributed to the effects of interannual variation in WTD on that of NEP. *Ecosys* simulated a site measured gradual drawdown of average growing season (May-August) WTD well from 2004 to 2009 (Fig. 7d) (Mezbahuddin et al., 2016). A small WTD drawdown simulated a large increase in growing season GPP from 2004 to 2005 as corroborated by similar increase in EC-derived GPP (Fig. 7b). This increase in GPP was also contributed by a larger GPP in May 2005 which was warmer than May 2004. This small WTD drawdown, however, did not raise either modelled or EC-derived growing season R_e from 2004 to 2005 (Fig. 7c). June and July of 2005 was cooler than 2004 by over 2°C which caused cooler soil that reduced R_e in 2005. Reduction in R_e in June-July 2005 due to cooler soil more than fully offset the increase in R_e due to the small WTD drawdown and resulted in modelled and EC-derived R_e that were smaller in the growing season of 2005 than in 2004 (Fig. 7c). Larger GPP and smaller R_e gave rise to modelled and EC-gap filled growing season NEP estimates that were larger in 2005 than those in 2004 (Fig. 7a).

WTD drawdown from 2005 to 2006 raised both modelled and EC-derived growing season GPP and R_e (Figs. 7b-c). Warmer growing season in 2006 caused warmer soil that further

624 contributed to the increase in modelled and EC-derived growing season R_e from 2005 with
 625 shallower WT to 2006 with deeper WT (Figs. 5, 6 and 7c-d). An increase in growing season R_e
 626 that was greater than the increase in growing season GPP caused a decline in modelled and EC-
 627 derived growing season NEP from 2005 to 2006 (Fig. 7a). Continued growing season WTD
 628 drawdown from 2006 to 2008 caused similar increases in modelled growing season GPP and R_e
 629 and hence no significant change in modelled growing season NEP (Figs. 7a-d). With this
 630 continued WTD drawdown from 2006 to 2008, however, EC-derived growing season GPP
 631 increased more than EC-derived growing season R_e that resulted a larger EC-derived NEP in the
 632 growing season of 2008 than in 2006 (Figs. 7a-d). A further drawdown in WTD from the
 633 growing season of 2008 to that of 2009 caused reductions in both modelled and EC-derived
 634 growing season GPP and R_e (Figs. 7a-d). Reductions in GPP and R_e from 2008 to 2009 was also
 635 contributed by lower T_a in 2009 than in 2008 that caused cooler canopies and soil (Figs. 7b-d).
 636 The reduction in EC-derived growing season GPP was larger than that in EC-derived growing
 637 season R_e thereby causing a decrease in growing season EC-gap filled NEP from 2008 to 2009
 638 (Figs. 7a- c). On the contrary, the reduction in modelled growing season GPP was smaller than
 639 the reduction in modelled R_e that yielded an increase in modelled growing season NEP from
 640 2008 to 2009 (Figs. 7a-c).

641 Modelled and EC-derived estimates of growing season GPP and R_e in 2009 were larger
 642 than those in 2004 despite similar mean T_a in those years (Figs. 7a-d). It suggested that increases
 643 in growing season GPP and R_e from 2004 to 2009 was a net effect of the deepening of average
 644 growing season WT (Figs. 7a-d). It was further corroborated by polynomial regressions of
 645 modelled growing season estimates of GPP and R_e against modelled average growing season
 646 WTD, and similar regressions of EC-derived growing season GPP and R_e against site measured

average growing season WTD (Figs. 8a-c). These relationships showed that there were increases in modelled and EC-derived growing season GPP and R_e with deepening of the growing season WT from 2004 to 2008 after which further WTD drawdown in 2009 started to cause slight declines in both GPP and R_e (Figs. 8b-c). Neither modelled nor EC-gap filled estimates of growing season NEP yielded significant regressions when regressed against modelled and measured growing season WTD respectively (Fig. 8a). It indicated that similar increases in modelled and EC-derived growing season estimates of GPP and R_e with deepening of WT left no net effects of WTD drawdown on either modelled or EC-derived growing season NEP (Figs. 7a-d and 8a).

Similar to the growing season trend, drawdown of both measured and modelled WTD averaged over the ice free periods (May-October) from 2004 to 2008 generally stimulated annual modelled and EC-derived GPP and R_e (Figs. 7f, g, h and 8e, f). Similar increases in both modelled and EC-derived annual GPP and R_e with WTD drawdown left no net WTD effects on modelled and EC-gap filled annual NEP (Figs. 7e, 8d). Although modelled WTD effects on GPP, R_e and hence NEP corroborated well by EC-derived GPP, R_e and EC-gap filled NEP, the modelled values for growing season and annual GPP and R_e were consistently higher than the EC-derived estimates of those throughout the study period (Figs. 7b, c, f, g- and 8b, c, e, f).

Increased GPP with WTD drawdown (Figs. 7b, f and 8b, e) was modelled predominantly through increased root growth and uptake of nutrients and consequently improved leaf nutrient status and hence more rapid CO_2 fixation in vascular PFTs. Under shallow WT during the growing season of 2004, roots in modelled black spruce and tamarack PFTs hardly grew below 0.35 m from the hummock surface. Modelled root densities of both black spruce and tamarack were higher by 2-3 orders of magnitude in the top 0.19 m of the hummock (data not shown). A

670 WTD drawdown by $-0.4\text{--}0.35$ m from the growing season of 2004 to that of 2009 caused increase
671 in maximum modelled rooting depth in both PFTs (Table 2). Increased root growth in modelled
672 vascular PFTs augmented root surface area for nutrient uptake under deeper WT in the growing
673 season of 2009 than in 2004. Increased root surface area along with increased nutrient
674 availability due to more rapid mineralization with improved aeration as a result of WTD
675 drawdown from 2004 to 2009 caused improved root nutrient uptake in modelled vascular PFTs.
676 Increased root growth, nutrient availability and hence uptake due to WTD drawdown from the
677 growing season of 2004 to that of 2009 caused an increase in modelled foliar N concentrations in
678 black spruce, tamarack and dwarf birch PFTs driving the increases in GPP modelled over this
679 period (Figs. 7b, f and 8b, e) (Table 2).

680 3.5. Simulated drainage effects on WTD and NEP

681 Artificial drainage can drastically alter WTD in a peatland that can cause dramatic
682 changes in peatland NEP by shifting the balance between GPP and R_e . Projected growing season
683 WT was deeper by ~ 0.5 m and ~ 0.55 m respectively from those in the real-time simulation in
684 drainage cycles 1 and 2 in all the years from 2004 to 2009 (Fig. 9a). Modelled growing season
685 GPP increased with drainage-induced WTD drawdown up to ~ 0.5 m below the hollow surface
686 (~ 0.8 m below the hummock surface) below which GPP decreased (Figs. 9c, f). The WTD
687 drawdown affected modelled vascular and non-vascular growing season GPP quite differently.
688 Modelled growing season vascular GPP increased with WTD drawdown before it plateaued and
689 eventually decreased when WTD fell below ~ 0.6 m from the hollow surface (~ 0.9 m below the
690 hummock surface) (Figs. 10a, c, e). On the contrary, modelled non-vascular growing season GPP
691 continued to decrease with WTD drawdown below ~ 0.1 m from the hollow surface (~ 0.4 m
692 below the hummock surface) (Figs. 10a-b, d).

693 WTD drawdown due to simulated drainage not only affected modelled growing season
694 GPP but also affected, and was affected by, the associated change in transpiration from vascular
695 canopies. Deeper WTD_x in drainage cycle 1 caused larger hydraulic gradients and greater lateral
696 discharge thereby deepening the WT with respect to that in the real-time simulation (Figs.
697 ~~10a~~^{9a}). Larger GPP throughout the growing seasons of 2004-2007 in the drainage cycle 1 than in
698 the real-time simulation caused a greater vertical water loss through rapid transpiration from
699 vascular canopies that further contributed to this deepening of WT (Fig. 9~~c~~^b). However, greater
700 lateral water discharge in drainage cycle 2 caused by deeper WTD_x did not deepen the modelled
701 growing season WT much below that in cycle 1 (Fig. 9a). The larger lateral water loss through
702 discharge in drainage cycle 2 than in cycle 1 was mostly offset by slower vertical water losses
703 due to vascular plant water stress as indicated by smaller GPP in the drainage cycle 2 (Fig. 9~~c~~^b).
704 The changing feedbacks between WTD, and GPP and plant water relations in *ecosys* also
705 indicated the ability of the model to simulate hydrological self-regulation which is an important
706 characteristic of peatland eco-hydrology (Dise, 2009).

707 Modelled growing season R_e continued to increase with projected drainage driven WTD
708 drawdown (Figs. 9d, g). Reductions in modelled growing season R_e from drainage cycle 1 to 2
709 during 2006-2009 indicated R_e inhibition due to desiccation of near surface peat layers and
710 surface residues (Fig. 9d). Overall GPP increased more than R_e with drainage driven initial WTD
711 drawdown that caused a small increase in modelled growing season NEP (Figs. 9 b, e).
712 Continued drainage driven WTD drawdown, however, caused declines in GPP particularly in
713 model years of 2008 and 2009 (Figs. 9c). This decrease in GPP was also accompanied by
714 increased R_e thereby causing a decrease in NEP when WT fell below a threshold of about ~0.45
715 m from the hollow surface, particularly during the drier years (Figs. 9b-g). This projected

drainage effect on WTD and NEP may be transient. Long-term manipulation of WTD may produce different trajectories of WTD effects on C processes and plant water relations in northern boreal peatlands via vegetation adaptation and succession (Strack et al., 2006; Munir et al., 2014).

4. Discussion

4.1. Modelling WTD effects on northern boreal peatland NEP

Hourly modelled, EC measured, and chamber measured net ecosystem, and soil and understorey CO₂ fluxes, and modelled and EC-derived seasonal and annual NEP, GPP and R_e estimates showed that WTD drawdown raised both GPP and R_e at the WPL (Figs. 3-8). Similar increases in GPP and R_e with WTD drawdown yielded no net effect of WTD drawdown on NEP at the WPL during 2004-2009 (Figs. 7-8). Four central hypotheses ~~that~~which outlined how coupled eco-hydrology and biogeochemistry algorithms in *ecosys* would simulate and explain the mechanisms of these WTD effects on R_e , GPP and NEP at the boreal fen peatland under study are examined in details in the following sections of 4.1.1 to 4.1.4.

4.1.1. Hypothesis 1: Increase in R_e with WTD drawdown

Shallow WTD in *ecosys* caused shallow aerobic zone above WT and thicker anaerobic zone below the WT. In the shallow aerobic zone, peat O₂ concentration [O_{2s}] was well above the Michaelis-Menten constant for O₂ reduction ($K_m=0.064$ g m⁻³) and hence DOC oxidation and consequent microbial uptake and growth in *ecosys* was not much limited by [O_{2s}] (Eqs. A17a, C14c). On the contrary, [O_{2s}] in the thicker anaerobic zone below the WT was well below K_m so that DOC oxidation was coupled with DOC reduction by anaerobic heterotrophic fermenters, which yielded much less energy (4.4 kJ g⁻¹ C) than did DOC oxidation coupled with O₂ reduction (37.5 kJ g⁻¹ C) (Fig. 1) (Eq. A21). Lower energy yields in the thicker anaerobic zone

resulted in slower microbial growth (Eq. A25) and R_h (Eq. A13). Since the anaerobic zone in *ecosys* was thicker than the aerobic zone under shallow WT, lower modelled R_h in the anaerobic zone contributed to reduced modelled soil respiration and hence R_e that was corroborated by EC and chamber measurements at the WPL (Figs. 5-8) (Tables 1 and 2).

WTD drawdown in *ecosys* caused peat pore drainage and increased θ_g thereby deepening of the aerobic zone. It raised D_g (Eq. D44) and increased O_2 influxes into the peat (Fig. 5c) (Eqs. D42-D43). Increased O_2 influxes enhanced $[O_{2s}]$ and stimulated R_h (Eqs. A13, A20), soil respiration and hence R_e (Figs. 5-8). Rapid mineralization of DON and DOP due to improved $[O_{2s}]$ under deeper WT also raised aqueous concentrations of NH_4^+ , NO_3^- and $H_2PO_4^-$ (Eqs. C23a, c, e) that increased microbial nutrient availability, uptake (Eq. A22) and growth (Eq. A29) and further enhanced R_e (Fig. 1) (Figs. 5-8). Modelled R_e stimulation by improved peat oxygenation due to WTD drawdown was corroborated well by EC and chamber measurements at the site (Figs. 5-8) (Tables 1 and 2). However, the chamber measured nighttime net CO_2 fluxes during warmer nights of 2006 with deeper WT were sometimes as large as corresponding EC-measured net ecosystem CO_2 fluxes (Figs. 5-6). Those very large chamber CO_2 effluxes could not be modelled to their full extent and consequently modelled vs. chamber CO_2 flux regression yielded a slope lower than 1 ± 0.1 in 2006 (Table 1c). Although modelled rate of increase in R_e with each 0.1 m of WTD drawdown was larger than EC-derived rate, it is still comparable with rates reported for other similar peatlands (Table 2). Kotowska (2013) carried out chamber based field measurements and laboratory incubation experiments in a moderately rich fen very close to our study site which reported that a WTD drawdown driven stimulation of aerobic microbial decomposition contributed to increased R_e . Mäkiranta et al. (2009) also found rapid microbial

decomposition in a Finish peatland due to thicker aerobic zone and consequently larger amounts of decomposable organic matter exposed to aerobic oxidation.

Apart from WTD, peat warming in *ecosys* also increased rates of decomposition (Eq. A1) through an Arrhenius function (Eq. A6) and increased R_h and R_e (Figs. 4-7). Warming effect on decomposition in *ecosys* was also modified by WTD. For a similar warming, greater thermal diffusivity in peat with deeper WT and consequent smaller water contents caused greater peat warming (Eqs. D34, D36). It enabled larger simulation of R_e during warming periods in 2006 and 2008 with deeper WT than in 2005 (Figs. 4-6). Increased stimulation of peat decomposition by warming under deeper WT was also modelled by Grant et al. (2012) using the same model *ecosys* over a northern fen peatland at Wisconsin, USA and by Ise et al. (2008) using a land surface scheme named ED-RAMS (Ecosystem Demography Model version 2 integrated with the Regional Atmospheric Modeling System) coupled with a soil biogeochemical model across several shallow and deep peat deposits in Manitoba, Canada.

4.1.2. Hypothesis 2: Increase in GPP with WTD drawdown

Modelled WTD variations influenced GPP by controlling root and microbial O_2 availability, energy yields, root and microbial growth and decomposition, rates of mineralization and hence root nutrient availability and uptake (Fig. 1). Wet soils under shallow WT caused low O_2 diffusion (Fig. 5c) (Eqs. D42-D44) into the peat and consequent low $[O_{2s}]$ meant that root O_2 demand had to be mostly met by $[O_{2r}]$. *Ecosys* inputs for root porosity ($\theta_{pr} = 0.1$) that governed O_2 transport through aerenchyma (Eq. D45) and hence maintained $[O_{2r}]$ was not enough to meet the root O_2 demand in saturated soil by the two over-storey tree PFTs i.e. black spruce and tamarack, causing shallow root systems to be simulated in these two tree PFTs under shallow WTD (Sec. 3.4). The under-storey shrub PFT (dwarf birch) had a higher root porosity ($\theta_{pr}=0.3$)

784 and hence had deeper rooting under shallow WT than the two tree PFTs (Sec. 3.4). Shallow
 785 rooting in the tree PFTs reduced root surface area for nutrient uptake. Root nutrient uptake (Eqs.
 786 C23b, d, f) in all the PFTs was also constrained by low nutrient availability due to smaller
 787 aqueous concentrations of NH_4^+ , NO_3^- and/or H_2PO_4^- (Eqs. C23a, c, e) resulting from slower
 788 mineralization (Eq. A26) of DON and DOP (Eq. A7) because of low $[\text{O}_{2s}]$ in the wet soils under
 789 shallow WT (Fig. 1). Slower root growth and nutrient uptake caused lower foliar σ_N and/or σ_P
 790 with respect to foliar σ_C (Eq. C11) that slowed the rates of carboxylation (Eq. C6) and hence
 791 reduced vascular GPP (Eq. C1) under shallow WT.

792 WTD drawdown enhanced O_2 diffusion (Fig. 5c) (Eqs. D42-D44) and raised $[\text{O}_{2s}]$ so that
 793 root O_2 demand in all the three vascular PFTs was almost entirely met by $[\text{O}_{2s}]$. Consequently
 794 roots in all the PFTs could grow deeper which increased the root surface for nutrient uptake
 795 (Table 2) (Sec. 3.4). Increase in modelled rooting depth due to WTD drawdown was
 796 corroborated well by studies on same PFTs as in our study grown on similar peatlands very close
 797 to the study site (Table 2). Murphy et al. (2009) found a significant increase in tree fine root
 798 production with WTD drawdown ~~from -0.1 to -0.25 m~~ by 0.15-0.2 m during a WTD
 799 manipulation study in a Finish peatland. Beside improved root growth, greater $[\text{O}_{2s}]$ under deeper
 800 WT also enhanced rates of mineralization (Eq. A26) of DON and DOP (Eq. A7) that raised
 801 aqueous concentrations of NH_4^+ , NO_3^- and/or H_2PO_4^- and hence facilitated root nutrient
 802 availability and uptake (Fig. 1). Enhanced root nutrient uptake increased foliar σ_N and/or σ_P with
 803 respect to foliar σ_C (Eq. C11) that hastened the rates of carboxylation (Eq. C6) and hence raised
 804 vascular GPP (Eq. C1) under deeper WT.

805 The three modelled vascular PFT were predominantly N limited as indicated by mass-
 806 based modelled foliar N to P ratios that matched well with site-measured mass-based foliar N to
 807 P ratios (Table 2). Mass-based modelled and measured foliar N to P ratio in all the PFTs were
 808 less than 16:1 indicating that the vegetation at the WPL was N limited (Aerts and Chapin III,
 809 1999). Since the modelled PFTs were predominantly N limited, increases in foliar N
 810 concentrations as a result of improved root nutrient availability, growth and nutrient uptake with
 811 WTD drawdown enhanced modelled carboxylation rates and hence modelled GPP. In a similar
 812 fen peatland close to our study site, Choi et al. (2007) found an increase in peat NO_3^- -N due to
 813 enhanced mineralization and nitrification stimulated by a WTD drawdown which improved
 814 foliar N status, and hence increased radial tree growth of black spruce and tamarack (Table 2).
 815 Macdonald and Lieffers (1990) also found improved foliar N concentrations in black spruce and
 816 tamarack trees that enhanced net photosynthetic C assimilation rates by those tree species in a
 817 northern Alberta moderately rich fen (Table 2). The rates of increases in foliar N concentrations
 818 in black spruce and tamarack trees due to WTD drawdown as reported in those studies are
 819 comparable with those in our modelled outputs (Table 2). Although modelled rate of increase in
 820 GPP with each 0.1 m of WTD drawdown was larger than EC-derived rate, it is still comparable
 821 with rates reported for other similar peatlands (Table 2).

822 **4.1.3. Hypothesis 3: Microbial water stress on R_e due to WT deepening below a threshold** 823 **WTD**

824 When modelled WTD fell below a threshold of ~ 0.3 m from the hollow surface (~ 0.6 m
 825 below the hummock surface), desiccation of the surface residue layer and near surface shallow
 826 peat layers reduced microbial access to substrate for decomposition (Eq. A15) which enabled
 827 simulation of reduced R_h in those layers. When reduction in surface residue and near-surface R_h

more than fully offset the increase in deeper R_h , net ecosystem R_h decreased. The offsetting effect on R_h partly contributed to simulated decrease in growing season $R_e (=R_h+R_a)$ from 2008 to 2009 with WTD drawdown that was corroborated by a similar decrease in EC-derived R_e (Fig. 7c). Greater reductions in R_h in desiccated surface residue and near surface peat layers also caused the reductions in growing season R_e in drainage cycle 2 from those in cycle 1 during 2007-2009 in the simulated drainage study (Fig. 9d). Similar to our study, Peichl et al. (2014) found reductions in R_e when WTD fell below a threshold of -0.325 m from the peat surface in a Swedish fen which could be partially attributed to reduction in near surface R_h due to desiccation. Mettrop et al. (2014) in a controlled incubation experiment found that the rates of microbial respiration in a nutrient rich Dutch fen initially increased with peat drying and consequent improved aeration. But excessive drying and consequent peat desiccation in their study reduced microbial respiration efficiency, growth and biomass. Dimitrov et al. (2010a) while modelling CO_2 exchange of a northern temperate bog using *ecosys* showed that a decrease in desiccated near surface peat respiration partially offset increased deeper peat respiration when WT deepened below a threshold of $-0.6-0.7$ m from the hummock surface.

4.1.4. Hypothesis 4: Plant water stress on GPP due to WT deepening below a threshold WTD

Modelled WTD drawdown below a threshold level also caused rapid peat pore drainage and low moisture contents in the near surface peat layers which were colonized by most of the vascular root systems and all of the belowground biomasses of non-vascular mosses (Eqs. D9-D29). When WTD fell below ~ 0.1 m from the hollow surface (~ 0.4 m below the hummock surface), vertical recharge through capillary rise from the WT was not adequate to maintain near surface peat moisture. It reduced peat water potential (ψ_s) and raised peat hydraulic resistance

851 (Ω_s) (Eq. B9) that suppressed root and moss water uptake (U_w) (Eq. B6) from desiccated near
 852 surface peat layers (Fig. 1). Since moss U_w entirely depended upon moisture supply from the
 853 near surface layers, reduction in U_w from desiccation of these layers caused reduction in moss
 854 canopy water potential (ψ_c) and hence moss GPP (Fig. 1) (Eqs. C1, C4) (Mezbahuddin et al.,
 855 2016). Reduction in root U_w from desiccated near surface layers, however, was offset by
 856 increased root U_w (Eq. B6) from deeper wetter layers, which had higher ψ_s and lower Ω_s , due to
 857 deeper root growth facilitated by enhanced aeration. It enabled the vascular PFTs in *ecosys* to
 858 sustain ψ_c , canopy turgor potential (ψ_A) (Eq. B4), stomatal conductance (g_c) (Eqs. B2, C4) and
 859 hence to sustain increased GPP (Eq. C1) due to higher root nutrient availability and uptake (Fig.
 860 1) (Mezbahuddin et al., 2016). Increased vascular GPP and consequent greater vascular plant
 861 growth further imposed limitations of water, nutrient and light to the modelled non-vascular
 862 PFTs due to interspecific competition and greater shading from the overstorey vascular PFTs.
 863 However, increases in vascular GPP due to enhanced plant nutrient status more than fully offset
 864 the suppression in moss GPP due to moss drying, and greater shading and competition from the
 865 overstorey, thereby causing a net increase in modelled GPP with WTD drawdown (Figs. 7b and
 866 10b-c). This simulation of increased vascular dominance over moss with deepening of WT was
 867 corroborated by several WTD manipulation studies (e.g., Moore et al., 2006, Munir et al., 2014)
 868 in similar peatlands in Alberta that reported increased tree, shrub and herb growths over mosses
 869 with WTD drawdown. However, increase in projected vascular GPP eventually plateaued and it
 870 started to decline when WT fell below ~0.6 m from the hollow surface (~0.9 m below the
 871 hummock surface) (Figs. 10c, e). It was because deeper root U_w (Eq. B6) could no longer offset
 872 suppression of near-surface root U_w when WT fell below threshold WTD, thereby causing lower
 873 ψ_c , ψ_A (Eq. B4), g_c (Eqs. B2, C4) and slower CO₂ fixation (Eq. C6) (Fig. 1).

874 These threshold WTD effects on modelled vascular and non-vascular plant water
 875 relations were validated well by testing modelled vs. site measured hourly energy fluxes (latent
 876 and sensible heat) and Bowen ratios, and modelled vs. site measured daily soil moisture at
 877 different depths throughout 2004-2009 as described in Mezbahuddin et al. (2016). Riutta et al.
 878 (2007) measured a reduction in moss productivity due to water limitation when WTD fell below
 879 ~0.15 m from the surface in a Finish fen peatland. However, they reported a sustained vascular
 880 GPP during that period indicating no vascular water stress (Riutta et al., 2007). Peichl et al.
 881 (2014) measured a reduction in moss GPP due to moss drying caused by insufficient moisture
 882 supply through capillary rise when WTD fell below ~~-0.253~~ m from the surface in a Swedish fen.
 883 Reductions in moss GPP due to decreased moss canopy water potentials were also modelled by
 884 Dimitrov et al. (2011) using the same model *ecosys* when WTD fell below ~~-0.3~~ m from the
 885 hummock surface of a Canadian temperate bog. They, however, found no vascular plant water
 886 stress and hence no reduction in vascular GPP during that period. Similarly, Kuiper et al. (2014)
 887 found reductions in moss productivity with peat drying while vascular productivity sustained in a
 888 simulated drought experiment on a Danish peat.

889 Continued deepening of WT can also cause vascular plant water stress and hence
 890 reductions in vascular GPP as projected in our drainage simulation (Figs. 10c, e). It can also be
 891 corroborated by field measurements across various northern boreal fen peatlands in Canada and
 892 Sweden. Sonnentag et al. (2010) found a reduction in stomatal conductance (g_c) of a canopy that
 893 included tamarack and dwarf birch and a consequent decline in GPP when WT fell below ~~-0.43~~
 894 m from the ridge surface at a fen peatland in Saskatchewan. Peichl et al. (2014) also found a
 895 reduction in vascular GPP due to plant water stress when WTD fell below ~~-0.3-25~~ m from the
 896 surface in a Swedish fen. The WTD threshold for reductions in vascular GPP in those two field

studies were shallower than that in our modelled projection i.e. ~0.6 m from the hollow surface (~0.9 m below the hummock surface) (Figs. 10a, c, e) thereby indicating different vertical rooting patterns determined by specific interactions between hydrologic properties and rooting. Lafleur et al. (2005) and Schwärzel et al. (2006) found much deeper WTD thresholds for reductions in vascular transpiration that could negatively affect vascular GPP over a Canadian pristine bog and a German drained fen respectively. Those WTD thresholds were ~0.65 and ~0.9 m below the surface for the pristine and drained peatland respectively, further indicating the importance of root-hydrology interactions and the resultant root adaptations, growth and uptake in determining WTD effects on vascular GPP across peatlands.

4.2. Divergences between modelled and EC-derived annual GPP, R_e and NEP

Modelled seasonal and annual GPP and R_e were consistently larger than EC-derived estimates of GPP and R_e during 2004-2009 (Figs. 7b, c, f, g). Although modelled annual GPP and R_e were larger than the EC-derived estimates, modelled annual NEP were consistently lower than the EC gap-filled annual NEP (Fig. 7e). Modelled annual NEP were smaller than EC-derived estimates because modelled R_e were larger than EC-derived estimates by margins bigger than by what modelled GPP were larger than EC-derived estimates (Figs. 7f-g). Modelled R_e were larger than EC-derived R_e estimates mainly due to the presence of gap filled night-time CO_2 fluxes ($=R_e$) in EC-derived estimates which were smaller than corresponding modelled values. It was apparent in negative intercepts that resulted from regressions of modelled vs. gap-filled net CO_2 fluxes (Table S1 in supplementary material). Gap filled R_e fluxes were calculated from soil temperature (T_s) at a shallow depth (0.05 m) (Sec. 2.2.2). During night-time and in the winter, peat at this shallow depth rapidly cooled down and yielded smaller night-time gap-filled CO_2 fluxes (Figs. 3, 5 and 6). On the contrary, corresponding modelled CO_2 effluxes were affected by

920 ~~temperatures of~~ not only the cooler shallow peat layers but also ~~the the-warmer~~ deeper peat
921 ~~profile layers and thus that were warmer than the shallower layers and thus~~ were larger than the
922 gap-filled fluxes (e.g., Figs. 5a, 6h-i). Like modelled CO₂ effluxes, chamber measured CO₂
923 effluxes in cooler nights also did not decline as rapidly as did the corresponding gap-filled CO₂
924 fluxes as night progressed which further indicated the likely contribution of gap-filling artifact to
925 CO₂ effluxes that were smaller than corresponding modelled fluxes (e.g., Figs. 5b vs. a, 6j-k vs.
926 g-h-i).

927 Systematic uncertainties embedded in EC methodology could also have contributed to
928 EC-derived annual and growing season R_e estimates which were smaller than the modelled
929 values (Figs. 7c, g). The major uncertainty in the EC methodology is the possible
930 underestimation of nighttime EC CO₂ flux measurements due to poor turbulent mixing under
931 stable air conditions (Goulden et al., 1997; Miller et al., 2004). On the contrary, modelled
932 biological production of CO₂ by plant and microbial respiration was independent of turbulent
933 mixing which ~~would-could~~ thus contribute to modelled R_e that were larger than EC-derived
934 estimates.

935 Complete energy balance closure in the model as opposed to incomplete (~75%) energy
936 balance closure in EC measurements would also give rise to modelled evapotranspiration and
937 GPP values that were larger than EC-derived estimates (Figs. 7b, f) (Mezbahuddin et al., 2016).
938 Modelled GPP influenced modelled R_e through root exudation and litter fall (Fig. 1). Therefore,
939 modelled GPP that were larger than EC-derived estimates would have further contributed to
940 modelled growing season and annual R_e estimates that were larger than EC-derived estimates
941 (Figs. 7c, g).

942 Modelled GPP and hence R_e can also be larger than EC-derived estimates due to
 943 uncertainties in model inputs for soil organic N, N deposition, N_2 fixation and any other sources
 944 of N inputs into the modelled ecosystem. In *ecosys*, plant productivity is governed by foliar N
 945 status which is constrained by root N availability and uptake. Our input for organic N into each
 946 modelled peat layer was measured for corresponding depth at the site (Fig. 2). To simulate N
 947 deposition, background wet deposition rates of 0.5 mg ammonium-N, and 0.25 mg nitrate-N per
 948 litre of precipitation ~~that-which~~ were reported for the study area were used as model inputs.
 949 However, from visual field observations, it was evident that there was a significant amount of
 950 nutrient inflow with the lateral water influxes into this fen peatland from the surrounding upland
 951 forests which was not quantified. To mimic this lateral nutrient inflow, we doubled the
 952 background wet deposition of NH_4^+ and NO_3^- as reported for the area and used these as ~~a~~
 953 surrogates of lateral nutrient inflow into the modelled ecosystem. *Ecosys* also included a N_2
 954 fixing algorithm which simulated symbiotic N_2 fixation in moss canopies that was reported for
 955 the boreal forests (Sec. 2.2.3). We tested the adequacy of these N inputs into the model by
 956 comparing modelled leaf N concentrations against those measured in the field. The modelled
 957 foliar N concentrations for ~~black spruce and tamarack~~the vascular PFTs corroborated well
 958 against site measurements (Table 2). To further examine the contribution of uncertainty due to
 959 model inputs towards the divergence between modelled and EC-derived seasonal and annual
 960 GPP and R_e , we performed a sensitivity test where we had a parallel run without doubling the
 961 background N wet deposition rates in the model, hence simulating no lateral N influx into the
 962 modelled ecosystem. Unlike the ~~current~~-run with lateral N inflow, the parallel run without lateral
 963 N inflow simulated GPP and R_e which were very close to the EC-derived estimates. However,
 964 the regressions between hourly modelled net CO_2 fluxes from the parallel run and EC-measured

hourly net CO₂ fluxes gave slopes of ~0.8 indicating under-simulation of the EC-measured fluxes in the parallel run with no lateral N inflow.

5. Conclusions

Our modelling study showed that, when adequately coupled into algorithms of a process-based ecosystem model, the existing knowledge of peatland eco-hydrological and peat biogeochemical processes could explain underlying mechanisms that governed WTD effects on net ecosystem CO₂ exchange of a boreal fen. Testing of our hypotheses against EC-measured net CO₂ fluxes, automated chamber fluxes and other biometric measurements at the site revealed that a drier weather driven WTD drawdown at this boreal fen raised both R_e and GPP due to improved aeration that facilitated 1) microbial and root O₂ availability, energy yields, growth and decomposition which raised microbial and root respiration; and 2) rapid nitrogen mineralization, and consequently increased root nitrogen availability and uptake that improved leaf nitrogen status and hence raised carboxylation (Figs. 1, 7-8) (Table 2). Similar increases in R_e and GPP with WTD drawdown to a certain depth caused no net WTD drawdown effect on NEP (Fig. 8). Modelled drainage projection, however, showed that further WTD drawdown caused by either drainage or climate change induced drying ~~could~~would cause plant water stress and reduce GPP and hence NEP of this boreal fen (Figs. 9-10). This study further reconciled and mechanistically explained the WTD effects on seasonal and annual GPP, R_e and hence NEP of this boreal fen which was previously speculated from EC-derived estimates. However, although modelled CO₂ fluxes were validated well by the EC and chamber measured net CO₂ fluxes, modelled values of annual and seasonal GPP and R_e were consistently larger than the EC-derived estimates (Table 1) (Figs. 7-8) (Sec. 4.2). These discrepancies between modelled and EC-derived GPP and R_e estimates also raised a potential research question of whether or not to use more robust process-

988 based estimates of these peatland C balance components instead of empirically modelled EC-
989 derived estimates that might not include some of the above discussed offsetting feedbacks in
990 peatland eco-hydrology and biogeochemistry.

991 The model algorithms that were used in this study represented coupled feedbacks among
992 ecosystem processes that governed carbon, water, energy, and nutrient (N, P) cycling in a
993 ~~peatland~~terrestrial ecosystem. These feedbacks were thus not parameterized for this particular
994 boreal fen peatland site. Instead, the modelled boreal fen was simulated from peatland specific
995 model inputs for weather, soil, and vegetation properties that had physical meaning and were
996 quantifiable at the site (Fig. 2). These modelled process level interactions were also validated by
997 corroborating modelled outputs against site measurements. On the contrary, most of the current
998 peatland C models uses scalar functions to represent these feedbacks and so those model
999 algorithms have to be parameterized for each peatland site. Therefore, the modelling approach as
1000 described in this study should be more robust than the scalar feedback approach while assessing
1001 WTD effects on peatland C balance under contrasting peat types, climates and hydrology, or
1002 under unknown future climates. These process level feedbacks are also scalable once the
1003 peatlands of interest are defined within the modelled landscapes by scalable model inputs for
1004 weather; peat hydrological, physical, and biological properties; and plant functional types (Sec.
1005 2.2.3). Current global land surface models either lack or have very poor representation of these
1006 feedbacks which is thus far limiting our large scale predictive capacity on WTD effects on boreal
1007 peatland C stocks. This modelling exercise would thus provide valuable information to improve
1008 representation of these feedbacks into next generation land surface models. Therefore, the
1009 insights gained from this modelling study should be a significant contribution to our

1010 understanding and apprehension of how peatlands would behave with changing hydrology under
1011 future drier and warmer climates.

1012 **Code availability**

1013 The *ecosys* model codes are listed in equation forms and sufficiently described in the
1014 supplementary material. The model codes that were written in FORTRAN will also be available
1015 on request from either symon.mezbahuddin@gov.ab.ca or rgrant@ualberta.ca.

1016 **Data availability**

1017 Field data that were used to validate model outputs are available at

1018 <http://fluxnet.ornl.gov/site/292>.

1019 **Author contribution**

1020 M. Mezbahuddin contributed to the model code modification and development, designing
1021 modelling experiment, simulation, validation, and analyses of modelled outputs. R. F. Grant is
1022 the original developer of the model *ecosys* and also contributed into simulation design and model
1023 runs. L. B. Flanagan was site principal investigator who led the collection, and quality control of
1024 the field data that were used to validate model outputs. M. Mezbahuddin wrote the manuscript
1025 with significant contributions from R. F. Grant and L. B. Flanagan.

1026 **Acknowledgments**

1027 Computing facilities for the modelling project was provided by Compute Canada,
1028 Westgrid, and University of Alberta. Funding for the modelling project was provided by several
1029 research awards from Faculty of Graduate Studies and Research and Department of Renewable
1030 Resources of University of Alberta and a Natural Sciences and Engineering Research Council
1031 (NSERC) of Canada discovery grant. The field research was carried out as part of the Fluxnet-
1032 Canada Research Network and the Canadian Carbon Program and was funded by grants to
1033 Lawrence B. Flanagan from NSERC, Canadian Foundation for Climate and Atmospheric
1034 Sciences, and BIOCAP Canada.

1035 **References**

- 1036 Aerts, R. and Chapin III, F.: The mineral nutrition of wild plants revisited: a re-evaluation of
1037 processes and patterns, *Adv. Ecol. Res.*, 30, 1-67, doi:10.1016/S0065-2504(08)60016-1,
1038 1999.
- 1039 Baker, I. T., Prihodko, L., Denning, A. S., Goulden, M., Miller, S., and Da Rocha, H. R.:
1040 Seasonal drought stress in the Amazon: reconciling models and observations, *J. Geophys.*
1041 *Res.-Biogeo.*, 113, G00B01, doi:10.1029/2007JG000644, 2008.
- 1042 Ballantyne, D. M., Hribljan, J. A., Pypker, T. G., and Chimner, R. A.: Long-term water table
1043 manipulations alter peatland gaseous carbon fluxes in Northern Michigan, *Wetl. Ecol.*
1044 *Manag.*, 22, 35-47, doi:10.1007/s11273-013-9320-8, 2014.
- 1045 Barr, A.G., Black, T.A., Hogg, E.H., Kljun, N., Morgenstern, K., and Nesic, Z.: Inter-annual
1046 variability in the leaf area index of a boreal aspen-hazelnut forest in relation to net
1047 ecosystem production, *Agric. For. Meteorol.* 126, 237-255,
1048 doi:10.1016/j.agrformet.2004.06.011, 2004.
- 1049 Bond-Lamberty, B., Gower, S. T., and Ahl, D. E.: Improved simulation of poorly drained forests
1050 using Biome-BGC, *Tree Physiol.*, 27, 703-715, doi:10.1093/treephys/27.5.703, 2007.
- 1051 Cai, T., Flanagan, L. B., and Syed, K. H.: Warmer and drier conditions stimulate respiration
1052 more than photosynthesis in a boreal peatland ecosystem: analysis of automatic chambers
1053 and eddy covariance measurements, *Plant Cell Environ.*, 33, 394-407, doi:10.1111/j.1365-
1054 3040.2009.02089.x, 2010.

1055 Campbell, G. S.: A simple method for determining unsaturated conductivity from moisture
 1056 retention data, *Soil Sci.*, 117, 311-314, 1974.

1057 Choi, W. J., Chang, S. X., and Bhatti, J. S.: Drainage affects tree growth and C and N dynamics
 1058 in a minerotrophic peatland, *Ecology*, 88, 443-453, doi:10.1890/0012-
 1059 9658(2007)88[443:DATGAC]2.0.CO;2, 2007.

1060 Cronk, J. K. and Fennessy, M. S.: *Wetland plants: biology and ecology*, CRC press, 2001.

1061 Dimitrov, D. D., Grant, R. F., Lafleur, P. M., and Humphreys, E. R.: Modeling the effects of
 1062 hydrology on ecosystem respiration at Mer Bleue bog, *J. Geophys. Res.-Biogeo.*, 115,
 1063 G04043, doi:10.1029/2010JG001312, 2010a.

1064 Dimitrov, D. D., Grant, R. F., Lafleur, P. M., and Humphreys, E. R.: Modelling subsurface
 1065 hydrology of Mer Bleue bog, *Soil Sci. Soc. Am. J.*, 74, 680-694,
 1066 doi:10.2136/sssaj2009.0148, 2010b.

1067 Dimitrov, D. D., Grant, R. F., Lafleur, P. M., and Humphreys, E. R.: Modeling the effects of
 1068 hydrology on gross primary productivity and net ecosystem productivity at Mer Bleue bog,
 1069 *J. Geophys. Res.-Biogeo.*, 116, G04010, doi:10.1029/2010JG001586, 2011.

1070 Dise, N. B: Peatland response to global change, *Science*, 326, 810-811,
 1071 doi:10.1126/science.1174268, 2009.

1072 Flanagan, L. B. and Syed, K. H.: Stimulation of both photosynthesis and respiration in response
 1073 to warmer and drier conditions in a boreal peatland ecosystem, *Glob. Change Biol.*, 17,
 1074 2271-2287, doi:10.1111/j.1365-2486.2010.02378.x, 2011.

1075 Frolking, S., Roulet, N. T., Moore, T. R., Lafleur, P. M., Bubier, J. L., and Crill, P. M.:
 1076 Modelling the seasonal to annual carbon balance of Mer Bleue bog, Ontario, Canada,
 1077 Global Biogeochem. Cy., 16, 1-21, doi:10.1029/2001GB001457, 2002.

1078 Gerten, D., Schaphoff, S., Haberlandt, U., Lucht, W., and Sitch, S.: Terrestrial vegetation and
 1079 water balance-hydrological evaluation of a dynamic global vegetation model, J. Hydrol.,
 1080 286, 249-270, doi:10.1016/j.jhydrol.2003.09.029, 2004.

1081 Gorham, E: Northern peatlands: role in the carbon cycle and probable responses to climatic
 1082 warming, Ecol. Appl., 1, 182-195, doi: 10.2307/1941811, 1991.

1083 Goulden, M. L., Daube, B. C., Fan, S. M., Sutton, D. J., Bazzaz, A., Munger, J. W., and Wofsy,
 1084 S. C.: Physiological responses of a black spruce forest to weather, J. Geophys. Res.-
 1085 Atmos., 102, 28987-28996, doi:10.1029/97JD01111, 1997.

1086 Grant, R. F., Desai, A. R., and Sulman, B. N.: Modelling contrasting responses of wetland
 1087 productivity to changes in water table depth, Biogeosciences, 9, 4215-4231,
 1088 doi:10.5194/bg-9-4215-2012, 2012.

1089 Ise, T., Dunn, A. L., Wofsy, S. C., and Moorcroft, P. R.: High sensitivity of peat decomposition
 1090 to climate change through water-table feedback, Nat. Geosci., 1, 763-766,
 1091 doi:10.1038/ngeo331, 2008.

1092 Kotowska, A: The long-term effects of drainage on carbon cycling in a boreal fen, M.Sc. thesis,
 1093 Department of Integrative Biology, University of Guelph, Ontario, Canada, 75 pp., 2013.

1094 Krinner, G., Viovy, N., de Noblet-Ducoudré, N., Ogée, J., Polcher, J., Friedlingstein, P., Ciais,
 1095 P., Sitch, S., and Prentice, I. C.: A dynamic global vegetation model for studies of the

1096 coupled atmosphere-biosphere system, *Global Biogeochem. Cy.*, 19, GB1015,
1097 doi:10.1029/2003GB002199, 2005.

1098 Kuiper, J. J., Mooij, W. M., Bragazza, L., and Robroek, B. J.: Plant functional types define
1099 magnitude of drought response in peatland CO₂ exchange, *Ecology*, 95, 123-131,
1100 doi:10.1890/13-0270.1, 2014.

1101 Lafleur, P. M., Hember, R. A., Admiral, S. W., and Roulet, N. T.: Annual and seasonal
1102 variability in evapotranspiration and water table at a shrub-covered bog in southern
1103 Ontario, Canada, *Hydrol. Process.*, 19, 3533-3550, 2005, doi: 10.1002/hyp.5842.

1104 Lieffers, V. J. and Rothwell, R. L.: Rooting of peatland black spruce and tamarack in relation to
1105 depth of water table, *Can. J. Botany*, 65, 817-821, doi: 10.1139/b87-111, 1987.

1106 Limpens, J., Berendse, F., Blodau, C., Canadell, J. G., Freeman, C., Holden, J., Roulet, N.,
1107 Rydin, H., and Schaepman-Strub, G.: Peatlands and the carbon cycle: from local processes
1108 to global implications – a synthesis, *Biogeosciences*, 5, 1475–1491, doi:10.5194/bg-5-
1109 1475-2008, 2008.

1110 Lizama, H. M. and Suzuki, I.: Kinetics of sulfur and pyrite oxidation by *Thiobacillus*
1111 thiooxidans. Competitive inhibition by increasing concentrations of cells, *Can. J.*
1112 *Microbiol.*, 37, 182-187, doi:10.1139/m91-028, 1991.

1113 Long, K. D., Flanagan, L. B., and Cai, T.: Diurnal and seasonal variation in methane emissions
1114 in a northern Canadian peatland measured by eddy covariance, *Glob. Change Biol.* 16,
1115 2420-2435, doi:10.1111/j.1365-2486.2009.02083.x, 2010.

1116 Long, K. D.: Methane fluxes from a northern peatland: mechanisms controlling diurnal and
 1117 seasonal variation and the magnitude of aerobic methanogenesis, M.Sc. thesis, Department
 1118 of Biological Sciences, University of Lethbridge, Lethbridge, AB, Canada, 100 pp., 2008.

1119 Macdonald, S. E. and Lieffers, V. J.: Photosynthesis, water relations, and foliar nitrogen of *Picea*
 1120 *mariana* and *Larix laricina* from drained and undrained peatlands, *Can. J. Forest Res.*, 20,
 1121 995-1000, doi:10.1139/x90-133, 1990.

1122 Mäkiranta, P., Laiho, R., Fritze, H., Hytönen, J., Laine, J., and Minkkinen, K.: Indirect regulation
 1123 of heterotrophic peat soil respiration by water level via microbial community structure and
 1124 temperature sensitivity, *Soil Biol. Biochem.*, 41, 695-703,
 1125 doi:10.1016/j.soilbio.2009.01.004, 2009.

1126 Markham, J. H.: Variation in moss-associated nitrogen fixation in boreal forest stands, *Oecologia*
 1127 161, 353-359, doi: 10.1007/s00442-009-1391-0, 2009.

1128 Mettrop, I. S., Cusell, C., Kooijman, A. M., and Lamers, L. P.: Nutrient and carbon dynamics in
 1129 peat from rich fens and *Sphagnum*-fens during different gradations of drought, *Soil Biol.*
 1130 *Biochem.*, 68, 317-328, doi:10.1016/j.soilbio.2013.10.023, 2014.

1131 Mezbahuddin, M., Grant, R. F., and Hirano, T.: How hydrology determines seasonal and
 1132 interannual variations in water table depth, surface energy exchange, and water stress in a
 1133 tropical peatland: modeling versus measurements, *J. Geophys. Res.-Biogeo.*, 120, 2132-
 1134 2157, doi:10.1002/2015JG003005, 2015.

1135 Mezbahuddin, M., Grant, R. F., and Hirano, T.: Modelling effects of seasonal variation in water
 1136 table depth on net ecosystem CO₂ exchange of a tropical peatland, *Biogeosciences*, 11,
 1137 577-599, doi:10.5194/bg-11-577-2014, 2014.

1138 Mezbahuddin, M., Grant, R.F. and Flanagan, L.B.: Modeling hydrological controls on variations
 1139 in peat water content, water table depth, and surface energy exchange of a boreal western
 1140 Canadian fen peatland, *J. Geophys. Res.-Biogeo.*, 121, 2216-2242,
 1141 doi:10.1002/2016JG003501, 2016.

1142 Miller, S. D., Goulden, M. L., Menton, M. C., da Rocha, H. R., de Freitas, H. C., Figueira, A. M.
 1143 e. S., and de Sousa, C. A. D.: Biometric and micrometeorological measurements of tropical
 1144 forest carbon balance, *Ecol. Appl.*, 14, 114–126, doi:10.1890/02-6005, 2004.

1145 Moore, T. and Basiliko, N.: Decomposition in boreal peatlands, in: *Boreal peatland ecosystems*,
 1146 edited by: Wieder, R. K. and Vitt, D. H., Springer Science & Business Media, 125-143,
 1147 2006.

1148 Munir, T. M., Xu, B., Perkins, M., and Strack, M.: Responses of carbon dioxide flux and plant
 1149 biomass to water table drawdown in a treed peatland in northern Alberta: a climate change
 1150 perspective, *Biogeosciences*, 11, 807-820, doi:10.5194/bg-11-807-2014, 2014.

1151 Murphy, M., Laiho, R., and Moore, T. R.: Effects of water table drawdown on root production
 1152 and aboveground biomass in a boreal bog, *Ecosystems*, 12, 1268-1282,
 1153 doi:10.1007/s10021-009-9283-z, 2009.

1154 Parmentier, F. J. W., Van der Molen, M. K., de Jeu, R. A. M., Hendriks, D. M. D., and Dolman,
 1155 A. J.: CO₂ fluxes and evaporation on a peatland in the Netherlands appear not affected by

1156 water table fluctuations, *Agr. Forest Meteorol.*, 149, 1201-1208,
 1157 doi:10.1016/j.agrformet.2008.11.007, 2009.

1158 Peichl, M., Öquist, M., Löfvenius, M. O., Ilstedt, U., Sagerfors, J., Grelle, A., Lindroth, A., and
 1159 Nilsson, M. B.: A 12-year record reveals pre-growing season temperature and water table
 1160 level threshold effects on the net carbon dioxide exchange in a boreal fen, *Environ. Res. Lett.*, 9, 055006, doi:10.1088/1748-9326/9/5/055006, 2014.

1162 Preston, M. D., Smemo, K. A., McLaughlin, J. W., and Basiliko, N.: Peatland microbial
 1163 communities and decomposition processes in the James Bay Lowlands, Canada, *Front. Microbiol.*, 3, 70, doi:10.3389/fmicb.2012.00070, 2012.

1165 Richardson, A. D., Hollinger, D. Y., Burba, G. G., Davis, K. J., Flanagan, L. B., Katul, G. G.,
 1166 Munger, J. W., Ricciuto, D. M., Stoy, P. C., Suyker, A. E., Verma, S. B., and Wofsy, S. C.:
 1167 A multi-site analysis of random error in tower-based measurements of carbon and energy
 1168 fluxes, *Agr. Forest Meteorol.*, 136, 1-18, doi:10.1016/j.agrformet.2006.01.007, 2006.

1169 Rippey, J. F. and Nelson, P. V.: Cation exchange capacity and base saturation variation among
 1170 Alberta, Canada, moss peats, *HortScience*, 42, 349-352, 2007.

1171 Riutta, T., Laine, J., and Tuittila, E. S.: Sensitivity of CO₂ exchange of fen ecosystem
 1172 components to water level variation, *Ecosystems*, 10, 718-733, doi:10.1007/s10021-007-
 1173 9046-7, 2007.

1174 Riutta, T.: Fen ecosystem carbon gas dynamics in changing hydrological conditions, *Diss. For.*
 1175 67, Department of Forest Ecology, Faculty of Agriculture and Forestry, University of
 1176 Helsinki, 46pp., 2008.

1177 Schaefer, K., Collatz, G. J., Tans, P., Denning, A. S., Baker, I., Berry, J., Prihodko, L., Suits, N.,
1178 and Philpott, A.: Combined simple biosphere/Carnegie-Ames-Stanford approach terrestrial
1179 carbon cycle model, *J. Geophys. Res.-Biogeo.*, 113, G03034, doi:10.1029/2007JG000603,
1180 2008.

1181 Schwärzel, K., Šimunek, J., van Genuchten, M. T., and Wessolek, G.: Measurement and
1182 modeling of soil-water dynamics and evapotranspiration of drained peatland soils, *J. Plant*
1183 *Nutr. Soil Sci.*, 169, 762-774, doi:10.1002/jpln.200621992, 2006.

1184 Sonnentag, O., van der Kamp, G., Barr, A. G., and Chen, J. M.: On the relationship between
1185 water table depth and water vapour and carbon dioxide fluxes in a minerotrophic fen, *Glob.*
1186 *Change Biol.*, 16, 1762–1776, doi:10.1111/j.1365-2486.2009.02032.x, 2010.

1187 St-Hilaire, F., Wu, J., Roulet, N. T., Frohling, S., Lafleur, P. M., Humphreys, E. R., and Arora,
1188 V.: McGill wetland model: evaluation of a peatland carbon simulator developed for global
1189 assessments, *Biogeosciences*, 7, 3517–3530, doi:10.5194/bg-7-3517- 2010, 2010.

1190 Strack, M., Waddington, J. M., Rochefort, L., and Tuittila, E. S.: Response of vegetation and net
1191 ecosystem carbon dioxide exchange at different peatland microforms following water table
1192 drawdown, *J. Geophys. Res.-Biogeo.*, 111, G02006, doi:10.1029/2005JG000145, 2006.

1193 Sulman, B. N., Desai, A. R., Cook, B. D., Saliendra, N., and Mackay, D. S.: Contrasting carbon
1194 dioxide fluxes between a drying shrub wetland in Northern Wisconsin, USA, and nearby
1195 forests, *Biogeosciences*, 6, 1115-1126, doi:10.5194/bg-6-1115-2009, 2009.

1196 Sulman, B. N., Desai, A. R., Saliendra, N. Z., Lafleur, P. M., Flanagan, L. B., Sonnentag, O.,
1197 Mackay, D. S., Barr, A. G., and van der Kamp, G.: CO₂ fluxes at northern fens and bogs

1198 have opposite responses to inter-annual fluctuations in water table, *Geophys. Res. Lett.*, 37,
1199 L19702, doi:10.1029/2010GL044018, 2010.

1200 Sulman, B. N., Desai, A. R., Schroeder, N. M., Ricciuto, D., Barr, A., Richardson, A. D.,
1201 Flanagan, L. B., Lafleur, P. M., Tian, H., Chen, G., Grant, R. F., Poulter, B., Verbeeck, H.,
1202 Ciais, P., Ringeval, B., Baker, I. T., Schaefer, K., Luo, Y., and Weng, E.: Impact of
1203 hydrological variations on modeling of peatland CO₂ fluxes: Results from the North
1204 American Carbon Program site synthesis, *J. Geophys. Res.-Biogeo.*, 117, G01031,
1205 doi:10.1029/2011JG001862, 2012.

1206 Syed, K. H., Flanagan, L. B., Carlson, P. J., Glenn, A. J., and Van Gaalen, K. E.: Environmental
1207 control of net ecosystem CO₂ exchange in a treed, moderately rich fen in northern Alberta,
1208 *Agr. Forest Meteorol.*, 140, 97-114, doi:10.1016/j.agrformet.2006.03.022, 2006.

1209 Tian, H., Chen, G., Liu, M., Zhang, C., Sun, G., Lu, C., Xu, X., Ren, W., Pan, S., and Chappelka,
1210 A.: Model estimates of net primary productivity, evapotranspiration, and water use
1211 efficiency in the terrestrial ecosystems of the southern United States during 1895–2007,
1212 *Forest Ecol. Manag.*, 259, 1311-1327, doi:10.1016/j.foreco.2009.10.009, 2010.

1213 Turunen, J., Tomppo, E., Tolonen, K., and Reinikainen, A.: Estimating carbon accumulation
1214 rates of undrained mires in Finland-application to boreal and subarctic regions, *The*
1215 *Holocene*, 12, 69-80, 2002.

1216 Updegraff, K., Pastor, J., Bridgman, S. D., and Johnston, C. A.: Environmental and substrate
1217 controls over carbon and nitrogen mineralization in northern wetlands, *Ecol. Appl.*, 5, 151-
1218 163, doi:10.2307/1942060, 1995.

- 1219 van Genuchten, M. T.: A closed-form equation for predicting the hydraulic conductivity of
 1220 unsaturated soils, *Soil Sci. Soc. Amer. J.*, 44, 892-898, doi:
 1221 10.2136/sssaj1980.03615995004400050002x, 1980.
- 1222 Waddington, J. M., Morris, P. J., Kettridge, N., Granath, G., Thompson, D. K., and Moore, P. A.:
 1223 Hydrological feedbacks in northern peatlands, *Ecohydrology*, 8, 113-127,
 1224 doi:10.1002/eco.1493, 2015.
- 1225 Weng, E. and Luo, Y.: Soil hydrological properties regulate grassland ecosystem responses to
 1226 multifactor global change: A modeling analysis, *J. Geophys. Res.-Biogeo.*, 113, G03003,
 1227 doi:10.1029/2007JG000539, 2008.
- 1228 Wesely, M. L. and Hart, R. L.: Variability of short term eddy-correlation estimates of mass
 1229 exchange, in: *The ForestAtmosphere Interaction*, edited by: Hutchinson, B. A., Hicks, B.
 1230 B., and Reidel, D., 591-612, Dordrecht, 1985.
- 1231 Wu, J., Kutzbach, L., Jager, D., Wille, C., and Wilmking, M.: Evapotranspiration dynamics in a
 1232 boreal peatland and its impact on the water and energy balance, *J. Geophys. Res.-Biogeo.*,
 1233 115, G04038, doi:10.1029/2009JG001075, 2010.
- 1234 Zhang, Y., Li, C., Trettin, C. C., Li, H., and Sun, G.: An integrated model of soil, hydrology, and
 1235 vegetation for carbon dynamics in wetland ecosystems, *Global Biogeochem. Cy.*, 16, 9-1-
 1236 9-17, doi:10.1029/2001GB001838, 2002.

1237 **Figure captions**

1238 **Fig. 1.** Schematic diagram of *ecosys* algorithms representing coupled key eco-physiological and
 1239 biogeochemical (aerobic and anaerobic) processes, and plant water relations of a typical boreal
 1240 fen peatland ecosystem that are affected by water table depth (WTD) fluctuation. Ψ_a , Ψ_c , and Ψ_s
 1241 =atmospheric, canopy and soil water potentials; Ψ_r =vascular root or non-vascular belowground
 1242 water potential; r_c =canopy stomatal resistance [$=1/\text{canopy stomatal conductance } (g_c)$]; Ω_s =soil
 1243 hydraulic resistance; Ω_r =hydraulic resistance to water flow through plants; OM=organic matter;
 1244 DOC, DON, DOP=dissolved organic carbon, nitrogen, and phosphorus; POC = particulate
 1245 organic C; and POM = particulate organic matter

1246 **Fig. 2.** Layout for *ecosys* model run to represent biological, chemical and hydrological
 1247 characteristics of a Western Canadian fen peatland. Figure is not drawn to scale. $D_{\text{hum}} =$ depth
 1248 to the bottom of a layer from the hummock surface; $D_{\text{holl}} =$ depth to the bottom of a layer from
 1249 the hollow surface; TOC = total organic C (Flanagan and Syed, 2011); TN = total nitrogen
 1250 (Flanagan and Syed, 2011); TP = total phosphorus (Flanagan and Syed, 2011); CEC = Cation
 1251 exchange capacity (Rippy and Nelson, 2007); the value for pH was obtained from Syed et al.
 1252 (2006); $\text{WTD}_x =$ external reference water table depth representing average water table depth of
 1253 the adjacent ecosystem; $L_t =$ distance from modelled grid cells to the adjacent watershed over
 1254 which lateral discharge / recharge occurs

1255 **Fig. 3. (a, c, e, g, i, k)** 3-day moving averages of modelled and EC-gap filled net ecosystem
 1256 productivity (NEP) (Flanagan and Syed, 2011), and **(b, d, f, h, j, l)** hourly modelled and half
 1257 hourly measured water table depth (WTD) (Syed et al., 2006; Cai et al., 2010; Long et al., 2010;
 1258 Flanagan and Syed, 2011) from 2004 to -2009 at a Western Canadian fen peatland. A positive

1259 NEP means the ecosystem is a carbon sink and a negative NEP means the ecosystem is a carbon
1260 source. A negative WTD represents a depth below hummock/hollow surface and a positive WTD
1261 represents a depth above hummock/hollow surface

1262 **Fig. 4.** Half hourly measured **(a)** incoming shortwave radiation, and **(b)** air temperature (T_a); and
1263 **(c)** hourly modelled and half hourly measured water table depth (WTD) (Syed et al., 2006; Cai et
1264 al.; 2010, Long et al.; 2010, Flanagan and Syed, 2011) during August of 2005, 2006 and 2008 at
1265 a Western Canadian fen peatland. A negative WTD represents a depth below hummock/hollow
1266 surface and a positive WTD represents a depth above hummock/hollow surface. Grey arrows
1267 indicate nights with similar temperatures

1268 **Fig. 5. (a)** Half hourly EC-gap filled (Flanagan and Syed, 2011) and hourly modelled ecosystem
1269 net CO₂ fluxes, **(b)** half hourly automated chamber measured (Cai et al., 2010) and hourly
1270 modelled understorey and soil CO₂ fluxes, and **(c)** hourly modelled soil CO₂ and O₂ fluxes
1271 during August of 2005, 2006 and 2008 at a Western Canadian fen peatland. No chamber CO₂
1272 flux measurement was available for 2008. Bars represent standard errors of means of chamber
1273 CO₂ fluxes ($n=9$). A negative flux represents an upward flux or a flux out of the ecosystem and a
1274 positive flux represents a downward flux or a flux into the ecosystem. Grey arrows indicate
1275 nights with similar temperatures (Fig. 4)

1276 **Fig. 6. (a-c)** Half hourly observed air temperature (T_a), **(d-f)** hourly modelled and half hourly
1277 observed water table depth (WTD) (Syed et al., 2006; Cai et al., 2010; Long et al., 2010;
1278 Flanagan and Syed, 2011), **(g-i)** half hourly EC-gap filled (Flanagan and Syed, 2011) and hourly
1279 modelled ecosystem net CO₂ fluxes, **(j-l)** half hourly automated chamber measured (Cai et al.,
1280 2010) and hourly modelled understorey and soil CO₂ fluxes during July-August of 2005, 2006

Formatted: Subscript

Formatted: Font: Italic

1281 and 2008 at a Western Canadian fen peatland. No chamber CO₂ flux measurement was available
 1282 for 2008. Bars represent standard errors of means of chamber CO₂ fluxes ($n=9$). A negative flux
 1283 represents an upward flux or a flux out of the ecosystem and a positive flux represents a
 1284 downward flux or a flux into the ecosystem. A negative WTD represents a depth below
 1285 hummock/hollow surface and a positive WTD represents a depth above hummock/hollow
 1286 surface

1287 **Fig. 7.** Modelled and EC-derived (Flanagan and Syed, 2011) growing season (May-August)
 1288 sums of **(a)** net ecosystem productivity (NEP), **(b)** gross primary productivity (GPP), and **(c)**
 1289 ecosystem respiration (R_e) during 2004-2009; **(d)** observed mean growing season air temperature
 1290 (T_a) and measured and modelled average growing season water table depth (WTD) during 2004-
 1291 2009; Modelled and EC-derived (Flanagan and Syed, 2011) annual sums of **(e)** NEP, **(f)** GPP,
 1292 and **(g)** R_e during 2004-2008; and **(h)** observed mean annual T_a and measured and modelled
 1293 average WTD during ice free periods (May-October) of 2004-2008 at a Western Canadian fen
 1294 peatland. A negative WTD represents a depth below hollow surface and a positive WTD
 1295 represents a depth above hollow surface. A positive NEP means the ecosystem is a carbon sink.
 1296 Annual modelled vs. EC-gap filled NEP, GPP, R_e estimates for 2009 were not compared due to
 1297 the lack of flux measurements from September to December in that year.

1298 **Fig. 8.** Regressions ($P<0.001$) of growing season (May-August) sums of modelled and EC-
 1299 derived (Flanagan and Syed, 2011) **(a)** net ecosystem productivity (NEP), **(b)** gross primary
 1300 productivity (GPP), and **(c)** ecosystem respiration (R_e) on growing season averages of modelled
 1301 and observed water table depth (WTD) during 2004-2009; and regressions ($P<0.001$) of annual
 1302 sums of modelled and EC-derived (Flanagan and Syed, 2011) **(d)** NEP, **(e)** GPP and **(f)** R_e on
 1303 average modelled and measured WTD during ice free periods (May-October) of 2004-2008 at a

1304 Western Canadian fen peatland. A negative WTD represents a depth below hollow surface and a
1305 positive WTD represents a depth above hollow surface. A positive NEP means the ecosystem is
1306 a carbon sink

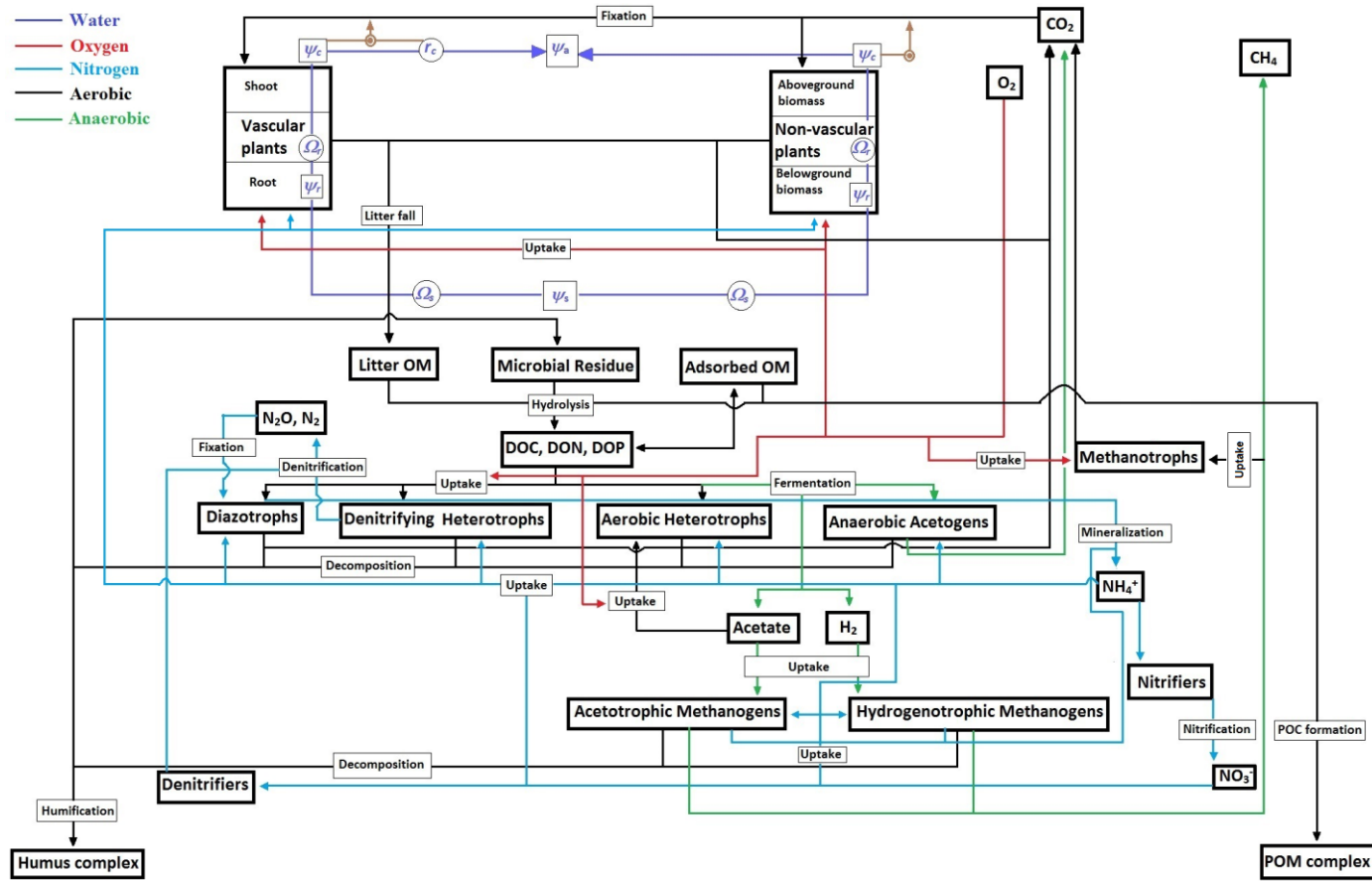
1307 **Fig. 9.** (a) Observed, ~~real-time~~ simulated (real-time simulation) and projected (drainage
1308 simulation) ~~drainage simulated~~ average growing season (May-August) water table depth (WTD);
1309 EC-derived, ~~real-time~~ simulated and projected ~~drainage simulated~~ growing season sums of (b)
1310 net ecosystem productivity (NEP), (c) gross primary productivity (GPP), and (d) ecosystem
1311 respiration (R_e); and regressions ($P < 0.001$) of ~~real-time~~ simulated and projected ~~drainage~~
1312 ~~simulated~~ sums of (e) NEP, (f) GPP, and (g) R_e on ~~real-time~~ simulated and projected ~~drainage~~
1313 ~~simulated~~ average growing season WTD during 2004-2009 at a Western Canadian fen peatland.
1314 A negative WTD represents a depth below hollow surface and a positive WTD represents a
1315 depth above hollow surface. A positive NEP means the ecosystem is a C sink

1316 **Fig. 10.** Simulated (real-time simulation) and projected (drainage simulation) ~~Real-time~~
1317 ~~simulated and projected drainage simulated~~ (a) average growing season (May-August) water
1318 table depth (WTD), (b) growing season sums of non-vascular (moss) gross primary productivity
1319 (GPP), and (c) growing season sums of vascular GPP; and regressions ($P < 0.001$) of ~~real-time~~
1320 simulated and projected ~~drainage simulated~~ sums of (d) non-vascular GPP, and (e) vascular GPP
1321 on ~~real-time~~ simulated and projected ~~drainage simulated~~ average growing season WTD during
1322 2004-2009 at a Western Canadian fen peatland. A negative WTD represents a depth below
1323 hollow surface and a positive WTD represents a depth above hollow surface

1324

Formatted: Space After: 10 pt, Line spacing: Double

— Water
 — Oxygen
 — Nitrogen
 — Aerobic
 — Anaerobic



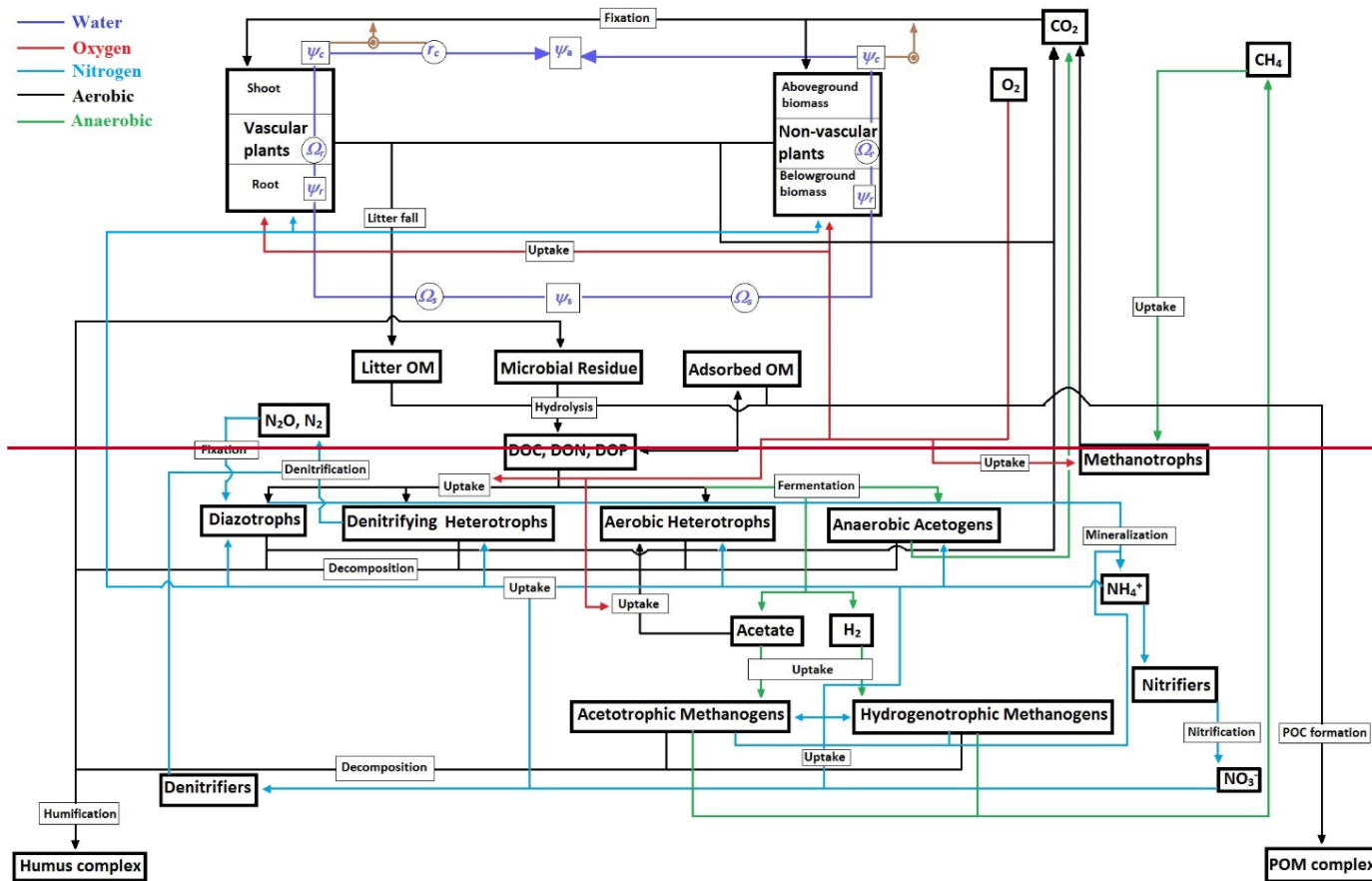
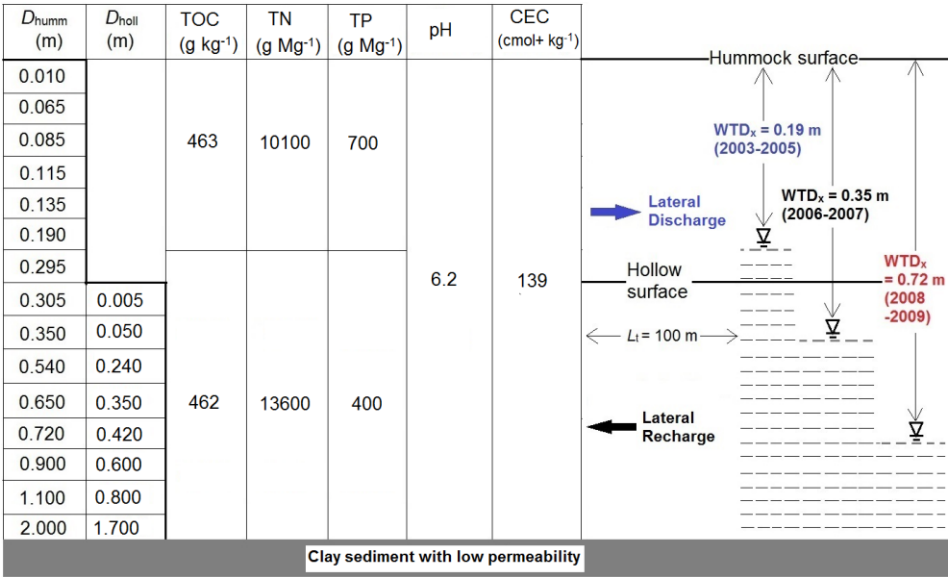


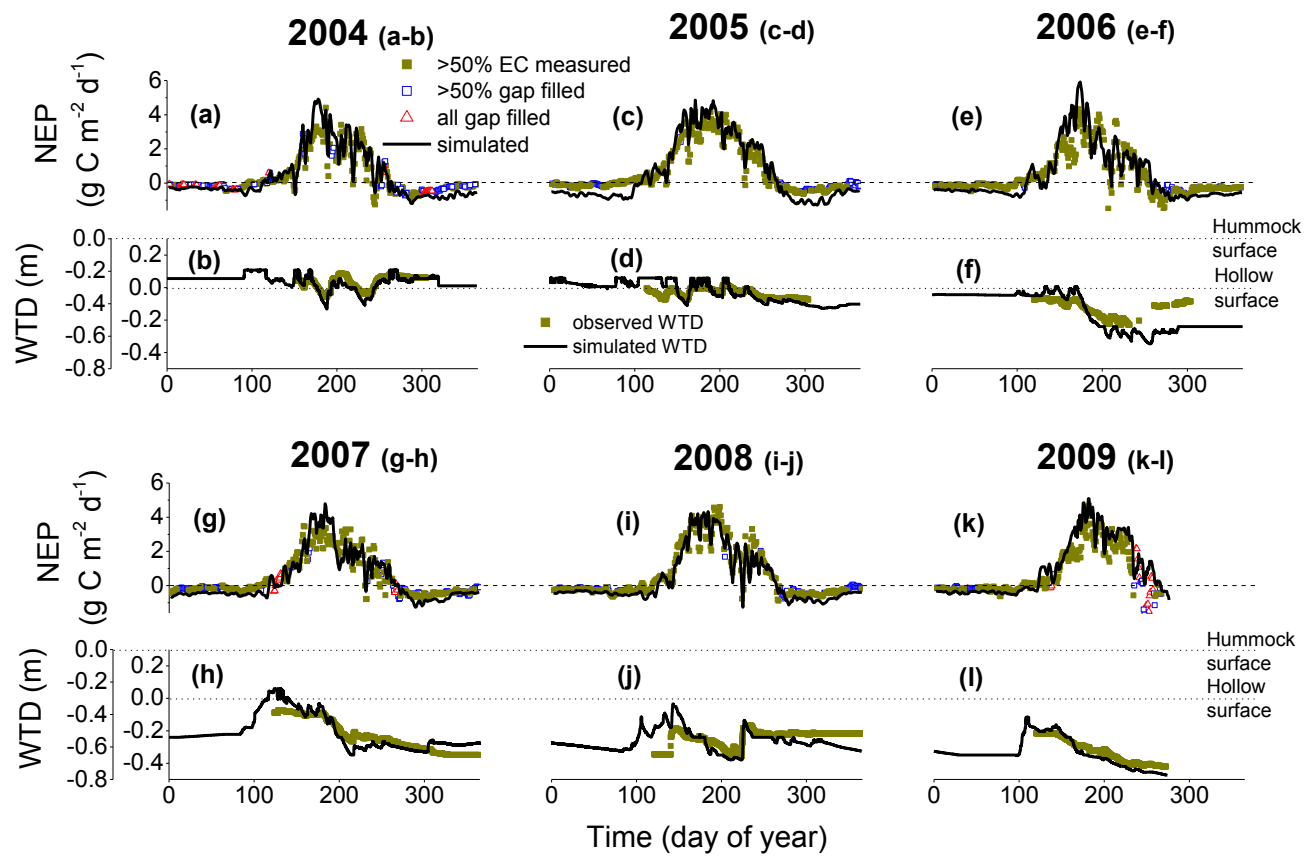
Fig. 1.

1328

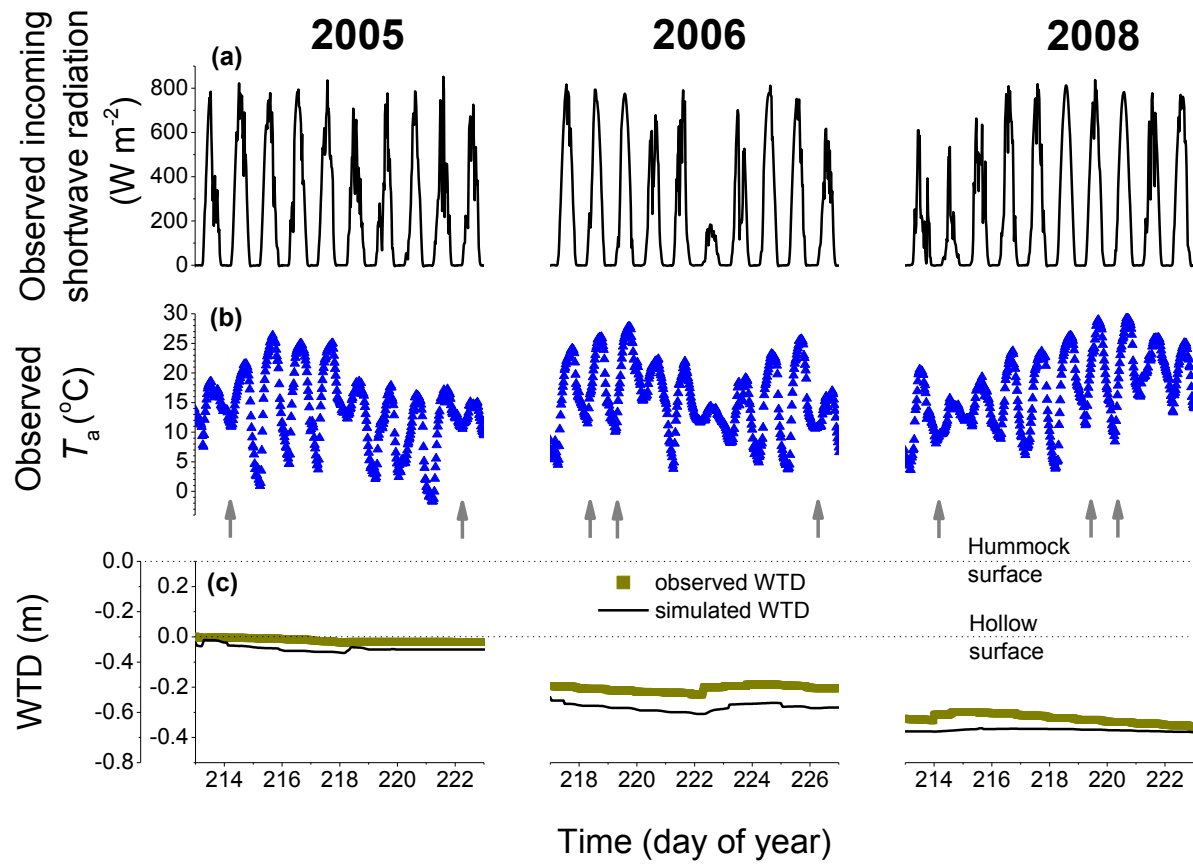


1329

1330 **Fig. 2.**



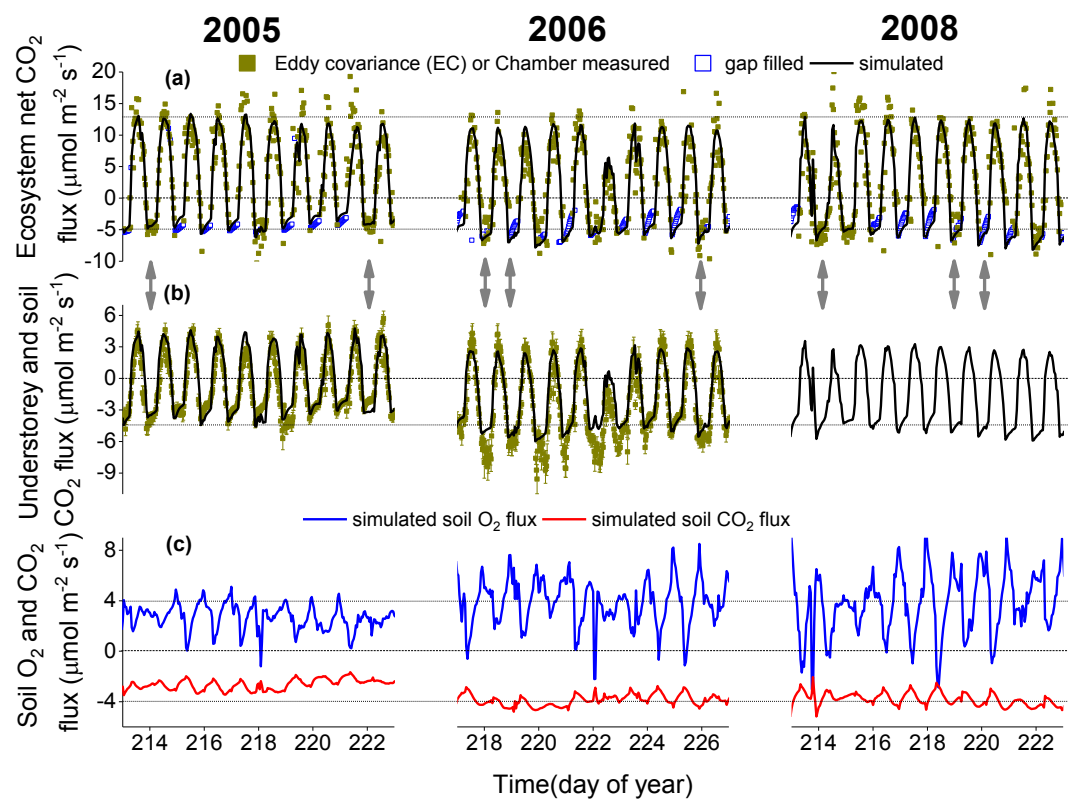
1331
1332 **Fig. 3.**



1333

1334 **Fig. 4.**

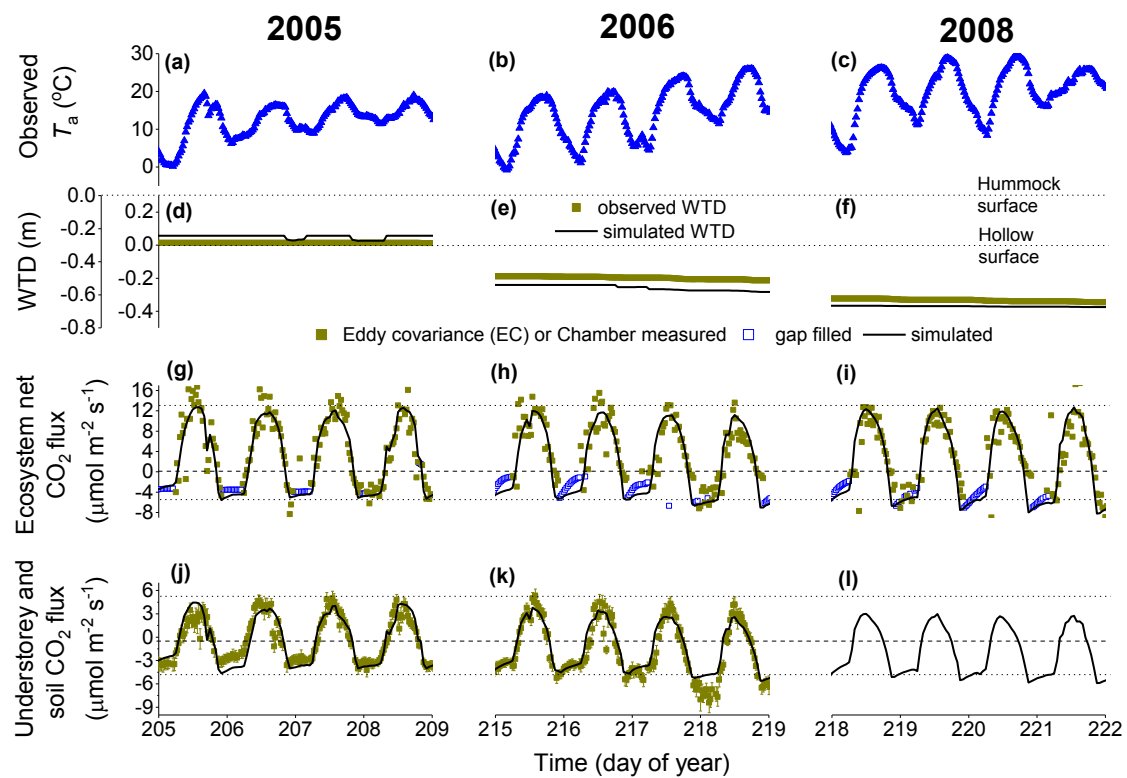
1335



1336

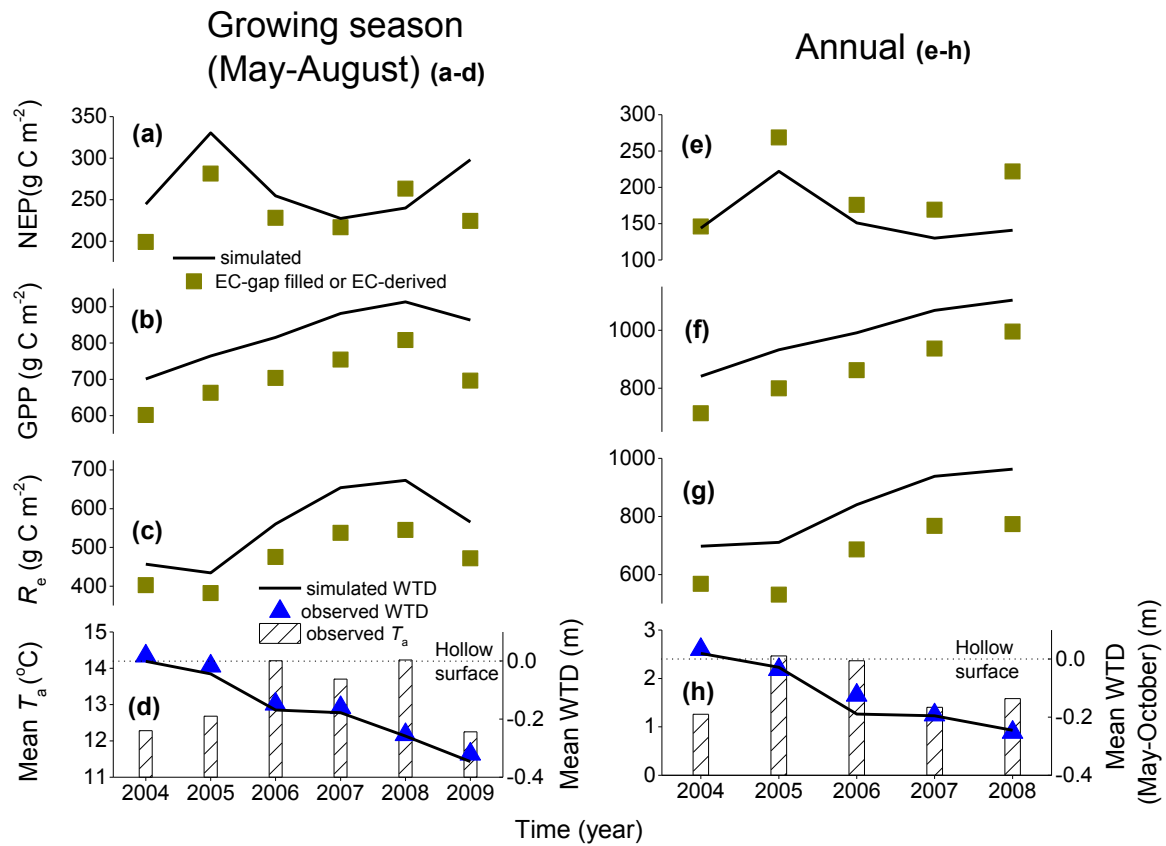
1337 **Fig. 5.**

1338



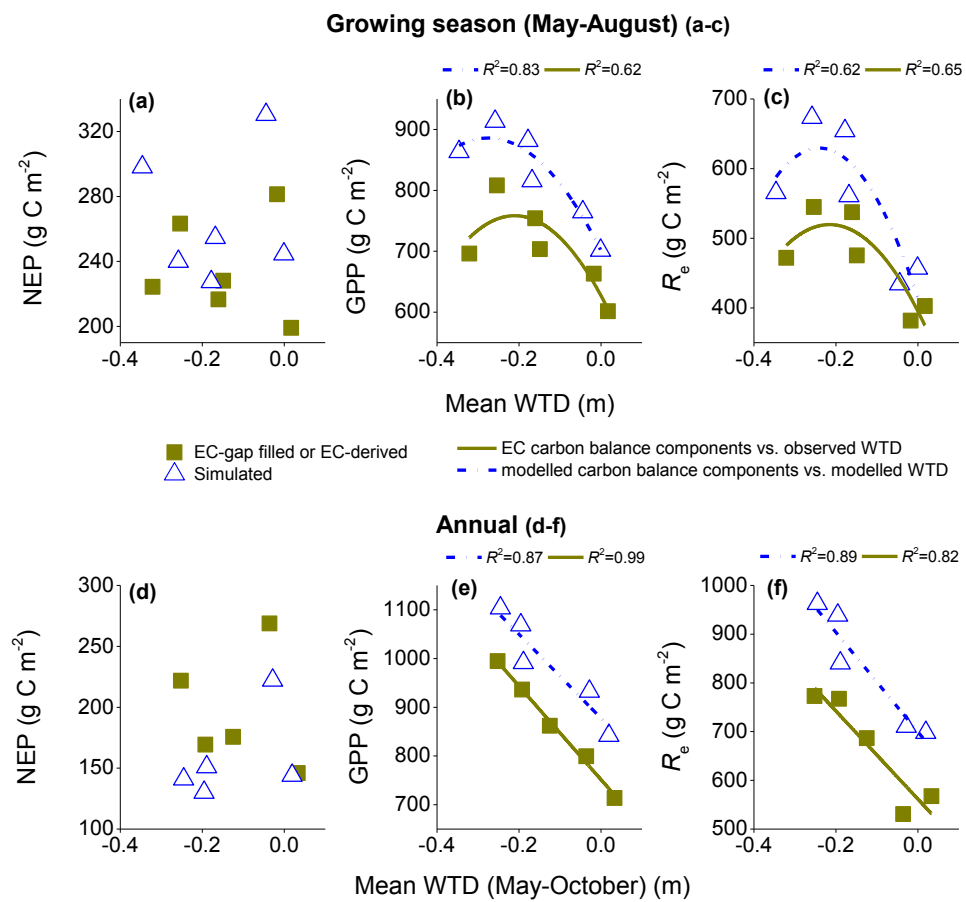
1339

1340 **Fig. 6.**



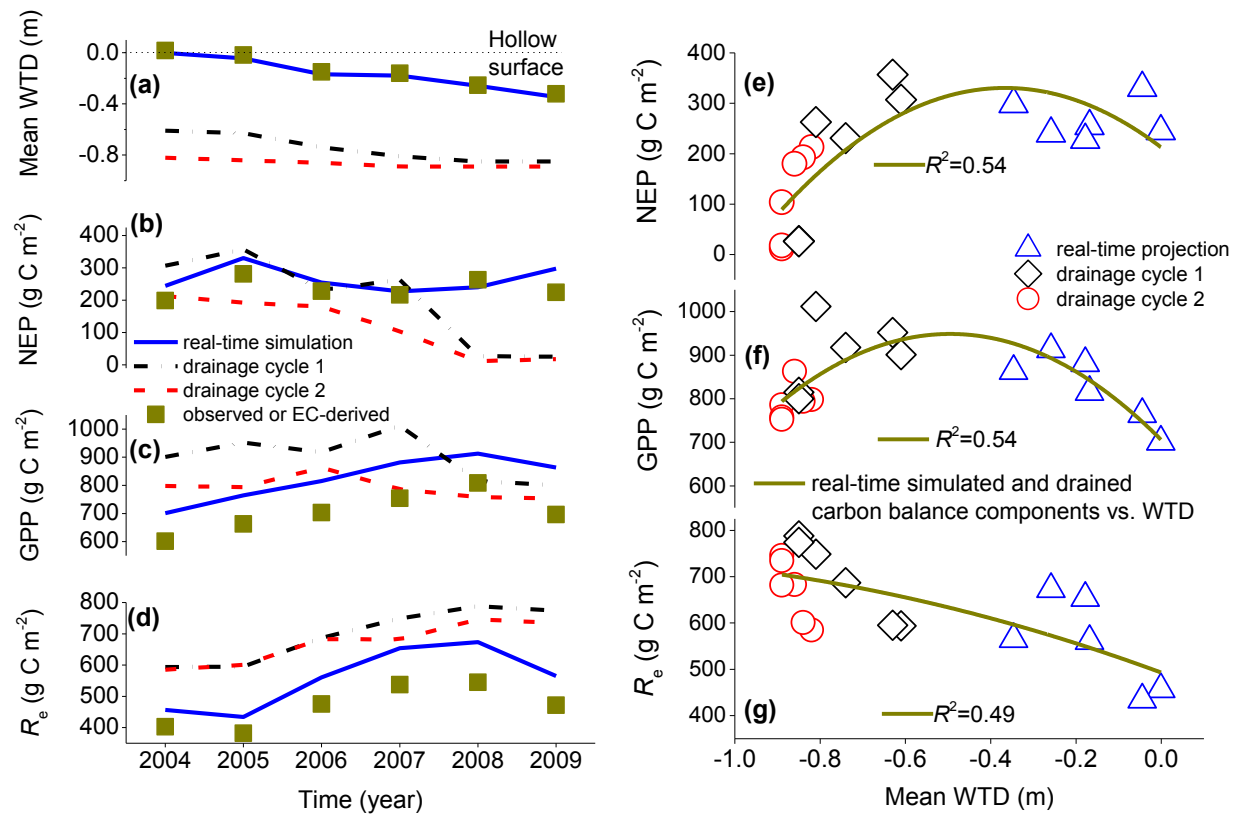
1341

1342 **Fig. 7.**



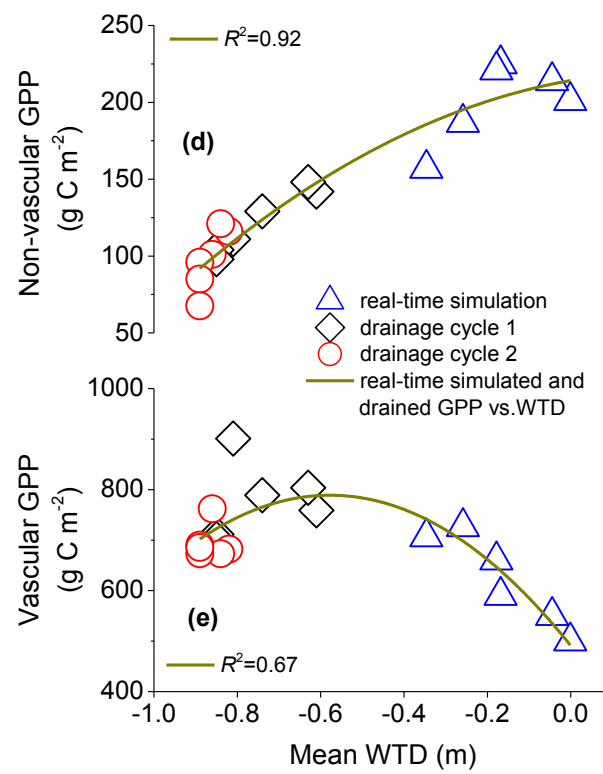
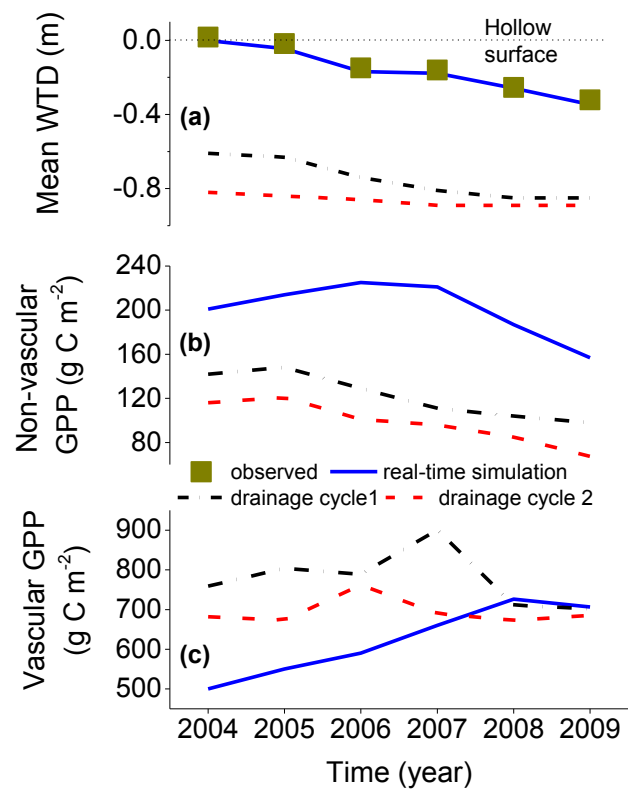
1343

1344 **Fig. 8.**



1345

1346 **Fig. 9.**



1347

1348 **Fig. 10.**

Table 1. Statistics from regressions between hourly modelled and measured net CO₂ fluxes from 2004-2009 at a Western Canadian fen peatland

(a) Regressions of modelled vs. EC measured (recorded at $u^* > 0.15 \text{ m s}^{-1}$) net ecosystem CO ₂ fluxes over whole years of 2004-2008 ^a							
Year	Total annual precipitation (mm)	<i>n</i>	<i>a</i>	<i>b</i>	<i>R</i> ²	RMSE (μmol m ⁻² s ⁻¹)	RMSRE (μmol m ⁻² s ⁻¹)
2004	553	5034	0.08±0.03	1.10±0.01	0.81	1.58	1.92
2005	387	5953	0.07±0.03	1.03±0.01	0.82	1.68	1.99
2006	465	6012	0.07±0.03	1.08±0.01	0.79	1.68	1.98
2007	431	5385	0.06±0.03	0.99±0.01	0.79	1.83	2.09
2008	494	5843	-0.01±0.02	0.98±0.01	0.84	1.63	2.02
(b) Regressions of modelled vs. EC measured (recorded at $u^* > 0.15 \text{ m s}^{-1}$) net ecosystem CO ₂ fluxes over growing seasons (May-August) of 2004-2009							
Year	Total growing season precipitation (mm)	<i>n</i>	<i>a</i>	<i>b</i>	<i>R</i> ²	RMSE (μmol m ⁻² s ⁻¹)	RMSRE (μmol m ⁻² s ⁻¹)
2004	287	2043	0.55±0.07	1.05±0.01	0.78	2.27	2.55
2005	276	2200	0.82±0.07	0.98±0.01	0.79	2.50	2.74
2006	253	2107	0.48±0.07	1.06±0.01	0.78	2.36	2.76
2007	237	1822	0.65±0.07	0.93±0.01	0.75	2.91	3.06
2008	276	2070	0.32±0.07	0.96±0.01	0.82	2.45	2.85
2009	138	1870	0.76±0.08	1.01±0.01	0.81	2.27	2.83
(c) Regressions of modelled vs. measured chamber net CO ₂ fluxes (understorey vegetation and soil CO ₂ fluxes) over ice free periods (May-October) of 2005-2006							

Formatted Table

Year	Mean May- October WTD (m)		<i>n</i>	<i>a</i>	<i>b</i>	<i>R</i> ²	RMSE (μmol m ⁻² s ⁻¹)	RMSRE (μmol m ⁻² s ⁻¹)
	<u>Mod elled</u>	<u>Meas ured</u>						
2005	<u>0.33</u>	<u>0.34</u>	<u>3285</u>	<u>0.43±0.02</u>	<u>1.05±0.01</u>	<u>0.68</u>	<u>1.19</u>	<u>2.38</u>
2006	<u>0.48</u>	<u>0.42</u>	<u>3855</u>	<u>0.31±0.03</u>	<u>0.85±0.01</u>	<u>0.71</u>	<u>1.44</u>	<u>3.25</u>
	<u>Mea sure d</u>	<u>Model led</u>						
2005	<u>0.34</u>	<u>0.33</u>	<u>3285</u>	<u>0.43</u>	<u>1.05</u>	<u>0.68</u>	<u>1.19</u>	<u>2.38</u>
2006	<u>0.42</u>	<u>0.48</u>	<u>3855</u>	<u>0.31</u>	<u>0.85</u>	<u>0.71</u>	<u>1.44</u>	<u>3.25</u>

WTD = water table depth below the hummock surface; (*a*, *b*) from simple linear regressions of modelled on measured (\pm standard errors), and *R*² = coefficient of determination; RMSE = root mean square for errors from simple linear regressions of measured on simulated; RMSRE= root mean square for random errors in measurements ~~from simple linear regressions of simulated on measured~~; RMSRE for eddy covariance (EC) measurements were ~~calculated~~ estimated by inputting EC CO₂ fluxes recorded at *u** (friction velocity) > 0.15 m s⁻¹ into algorithms for estimation of random errors due to EC CO₂ measurements developed for forests by Richardson et al. (2006);

^a whole year modelled vs. EC net CO₂ flux regression for 2009 could not be done due to the lack of flux measurements from September to December in that year.

Formatted: Font: Not Italic

Formatted: Font: Not Italic

Formatted: Font: Not Italic

Formatted: Font: Not Italic

Formatted: Font: Not Italic

Formatted: Font: Not Italic

Formatted: Font: Not Italic

Formatted: Font: Not Italic

Formatted: Line spacing: Multiple 1.15 li

Table 2. Effects of water table depth (WTD) drawdown on components of ecosystem carbon and nutrient cycles of a Western Canadian fen peatland

	Modelled	Eddy covariance-derived/biometrically measured at the site ^a	Values from other studies in similar peatlands
<u>Growing season (May to August) mean WTD drawdown from 2004 to 2009</u>	<u>from 0.3 m below the hummock surface (at the hollow surface) in 2004 to 0.65 m below the hummock surface (0.35 below the hollow surface) in 2009</u>	<u>from 0.32 m below the hummock surface (0.02 m below the hollow surface) in 2004 to 0.62 m below the hummock surface (0.32 m below the hollow surface) in 2009</u>	
Rate of increase in <u>annual</u> R_e with each 0.1 m of WTD drawdown	0.26 $\mu\text{mol CO}_2 \text{ m}^{-2} \text{ s}^{-1}$	0.16 $\mu\text{mol CO}_2 \text{ m}^{-2} \text{ s}^{-1}$	(1) -0.3 <u>-0.32 ± 0.27</u> $\mu\text{mol CO}_2 \text{ m}^{-2} \text{ s}^{-1}$ _b (2) -0.33 $\mu\text{mol CO}_2 \text{ m}^{-2} \text{ s}^{-1}$ ^e
Rate of increase in <u>growing season</u> GPP with each 0.1 m of WTD drawdown	0.39 $\mu\text{mol CO}_2 \text{ m}^{-2} \text{ s}^{-1}$	0.22 $\mu\text{mol CO}_2 \text{ m}^{-2} \text{ s}^{-1}$	(1) -0.3 <u>-0.32 ± 0.158</u> $\mu\text{mol CO}_2 \text{ m}^{-2} \text{ s}^{-1}$ _{l b} (2) -0.47 <u>-0.47 ± 0.064</u> $\mu\text{mol CO}_2 \text{ m}^{-2} \text{ s}^{-1}$ _{l c}

Formatted Table

Leaf nitrogen concentration (mid-July 2004)	Black Spruce	14.3 g N kg ⁻¹ C	12.4±0.6 g N kg ⁻¹ C
	Tamarack	32.1 g N kg ⁻¹ C	32.6±1.43 g N kg ⁻¹ C
	Dwarf Birch	37.4 g N kg ⁻¹ C	41.4±1.8 g N kg ⁻¹ C
Leaf nitrogen (N) to phosphorus (P) ratio (mid-July 2004)	Black Spruce	6.6:1	7.1:1
	Tamarack	5.2:1	6.3:1
	Dwarf Birch	4.8:1	
Increase in foliar nitrogen concentrations with WTD drawdown	Black Spruce	from 14.3 to 17.2 g N kg ⁻¹ C with the growing season WTD drawdown from 0.3 m below the hummock surface in 2004 to 0.65 m below the hummock surface in 2009a-WTD drawdown from -0.25 to -0.65 m below the hummock surface over the growing seasons of 2004-2009	(1) from -24.8±0.6 to -27±0.4 g N kg ⁻¹ C with a WTD drawdown from 0.24 to 0.7 m below peat surface ^d (2) from 18.7±0.05-19 to -21.3±0.06 g N kg ⁻¹ C for a WTD drawdown by -0.4-0.55 m ^e
	Tamarack	from 32.1 to 36.7.7 g N kg ⁻¹ C with a-the growing season WTD drawdown from -0.25-3 m below the hummock surface in 2004 to -0.65 m below the hummock surface in 2009below the hummock surface over the growing seasons of 2004-2009	(1) from -41.4±0.4 to -66.2±1.2 g N kg ⁻¹ C for a WTD drawdown from 0.24 to 0.7 m below peat surface ^d (2) from -35.9±0.16 to -41.72±0.18 g N kg ⁻¹ C for a WTD drawdown by 0.4-0.5 m-0.45 m ^e

	Dwarf Birch	from 37.4 to 45.1 g N kg ⁻¹ C with <u>the growing season WTD drawdown from 0.3 m below the hummock surface in 2004 to 0.65 m below the hummock surface in 2009</u> a WTD drawdown from -0.25 to -0.65 m below the hummock surface over the growing seasons of 2004-2009	
Increase in maximum rooting depth with WTD drawdown	Black spruce	from 0.35 to 0.65 m below the hummock surface <u>with the growing season WTD drawdown from 0.3 m below the hummock surface in 2004 to 0.65 m below the hummock surface in 2009</u> with a WTD drawdown from -0.25 to -0.65 m over the growing seasons of 2004-2009	from 0.1 to 0.6 m below peat <u>hummock</u> surface with a WTD drawdown from 0.1 to 0.7 m below hummock surface ^f
	Tamarack	from 0.35 to 0.65 m below the hummock surface <u>with the growing season WTD drawdown from 0.3 m below the hummock surface in 2004 to 0.65 m below the hummock surface in 2009</u> with a WTD drawdown from -0.25 to -0.65 m over the growing seasons of 2004-2009	from 0.2 to 0.6 m below peat <u>hummock</u> surface with a WTD drawdown from 0.1 to 0.6 m below hummock surface ^f

GPP=gross primary productivity; R_e = ecosystem respiration; ^a Syed et al. (2006), Flanagan and Syed (2011); ^b Peichl et al. (2012) for a Swedish fen; ^c Ballantyne et al. (2014) for a Michigan fen peatland complex that has similar peat and plant functional types as our study site; ^d Choi et al. (2007) for a central Alberta fen peatland located ~350 km to the southwest of the study site; ^e Macdonald and

Lieffers (1990) for a northern Alberta fen peatland located ~250 km to the northwest of the study site; ^f Lieffers and Rothwell (1987) for a northern Alberta fen peatland located ~250 km to the northwest of the study site

